Universität Hamburg
DER FORSCHUNG | DER LEHRE | DER BILDUNG

CFEL SCIENCE

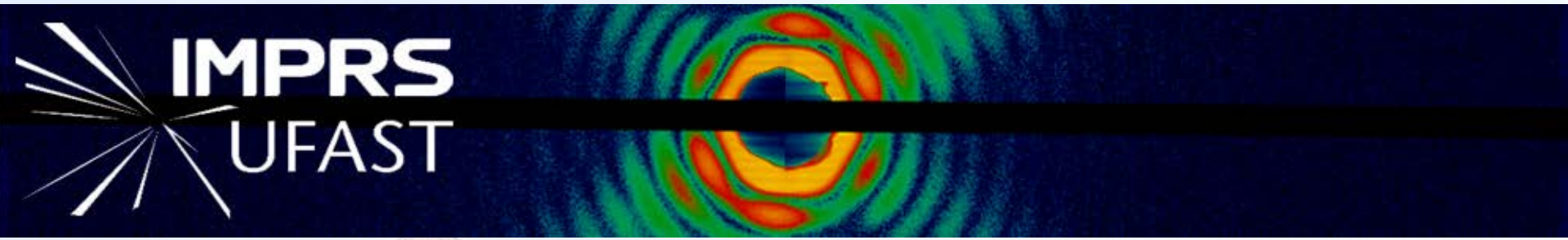

Course 2: Basic Technologies

Part II: X-ray optics

Jun.-Prof. Dr. Thorsten Uphues
Thorsten.Uphues@cfel.de

What do you see here?

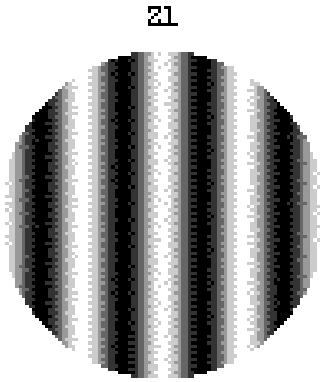

wavefront distortion

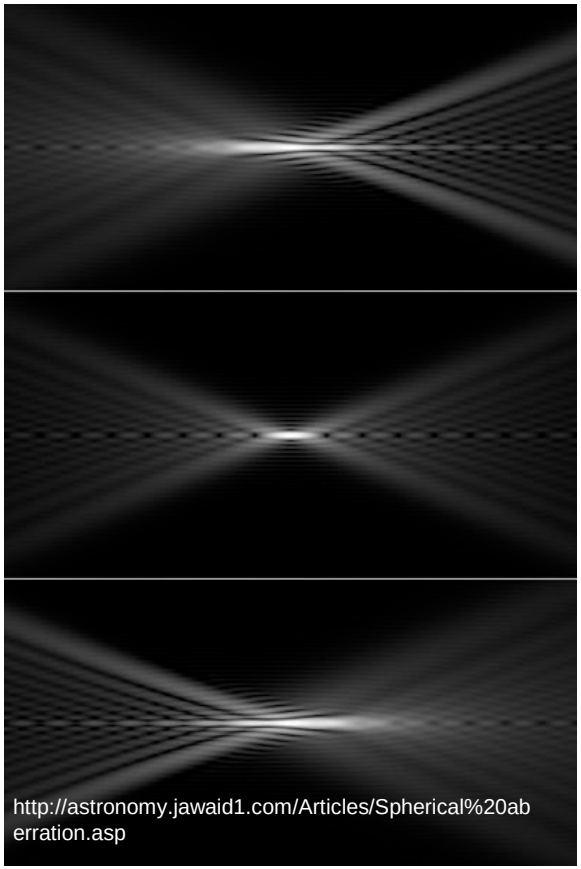

http://astronomy.jawaid1.com/Articles/Spherical%20aberration.asp

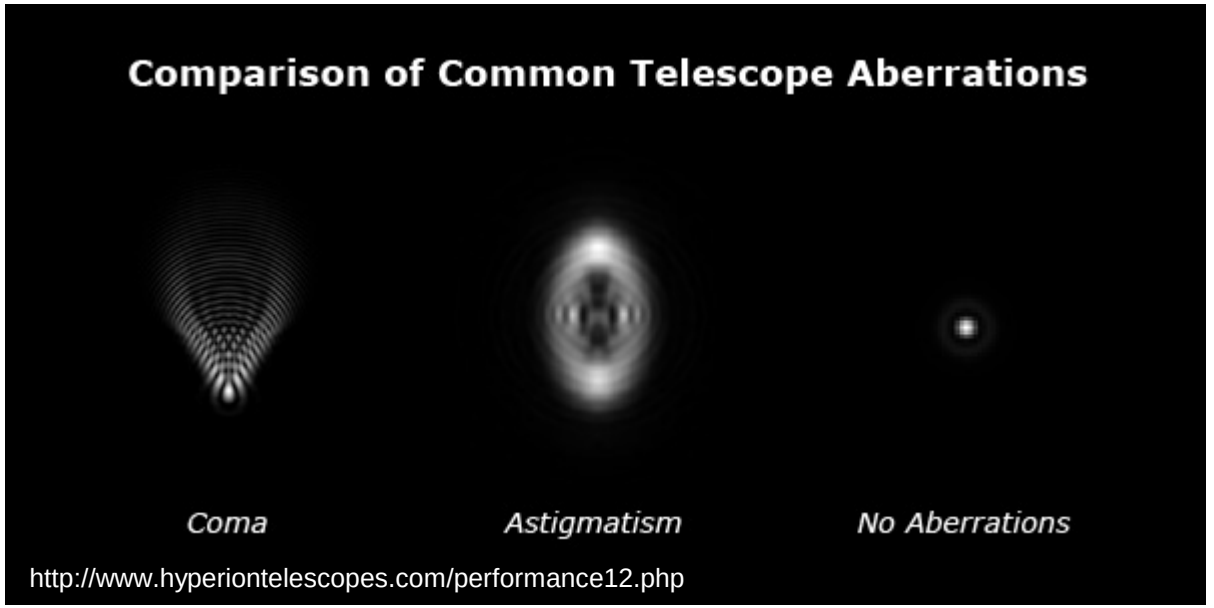

http://www.hyperiontelescopes.com/performance12.php

Frits Zernike

Physicist

Frits Zernike was a Dutch physicist and winner of the Nobel prize for physics in 1953 for his invention of the phase contrast microscope, an instrument that permits the study of internal cell structure ... Wikipedia

Born: July 16, 1888, Amsterdam

Died: March 10, 1966, Amersfoort

Education: Universiteit van Amsterdam

Awards: Nobel Prize in Physics, Rumford Medal

ASTIGMATISM.

In the case of an oblique bundle of rays impinging on the lens, as in Fig. 21, from a point not on the optical axis, the lens does not present a symmetrical front to the incident rays; as indicated in the figure, the lens appears foreshortened in the plane of incidence (containing optical axis PP' and point A; usually called *tangential* or *meridional* plane). The effect of the lens is to produce an emergent wave of less radius of curvature for

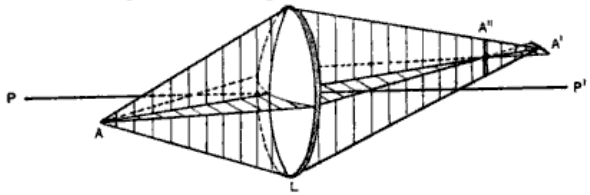

FIG. 21.

the tangential plane than for the plane normal to it (*sagittal plane*) (Figs. 21, 22*). The image formed in the tangential plane will then fall short of the image formed in the sagittal plane. The distance between the image points in the tangential and sagittal planes is the *astigmatic difference* and the aberration is called *astigmatism*. The total effect of astigmatism on an incident spherical wave is to produce an emergent wave of spherical front whose radius of curvature in the tangential plane is less or greater than that in

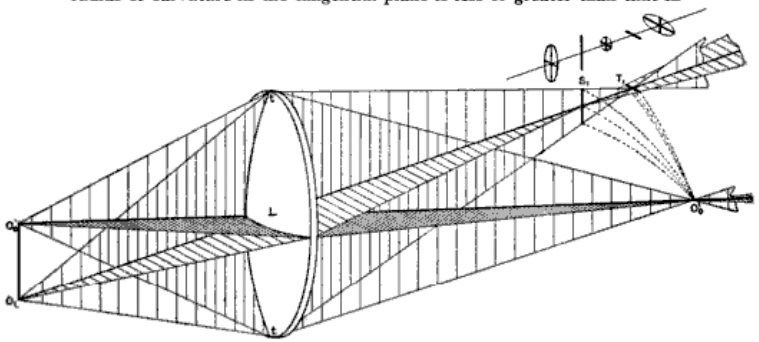

FIG. 22.

the sagittal plane; the practical consequence of this is that astigmatism produces from a plane object an image which consists of two coaxial warped and irregular surfaces. In correcting for astigmatism, the effort is made to make these two surfaces coincide for the useful field of the objective. Astigmatism is not, in general, very noticeable in microscopic objectives, because the inclination of the chief rays is comparatively small. It usually

*Fig. 22 was suggested to the writer by a drawing by Dr. H. Kellner, illustrating astigmatism.

Zernike Polynominals

The Zernike polynomials are a set of orthogonal polynomials that arise in the expansion of a wavefront function for optical systems with circular pupils.

The odd and even Zernike polynomials are given by

$$^{o}U_n^m(\rho,\phi) = R_n^m(\rho)\sin m\phi$$
$$^{e}U_n^m(\rho,\phi) = R_n^m(\rho)\cos m\phi$$

where the radial function $R_n^m(\rho)$ is defined for n and m integers with $n \geq m \geq 0$ by

$$R_n^m(\rho) = \begin{cases} \sum_{l=0}^{(n-m)/2} \dfrac{(-1)^l (n-l)!}{l!\left[\frac{1}{2}(n+m)-l\right]!\left[\frac{1}{2}(n-m)-l\right]!}\rho^{n-2l} & \text{for } n-m \text{ even} \\ 0 & \text{for } n-m \text{ odd} \end{cases}$$

Zernike polynominals II

Sometimes the Zernike polynominals are also denoted as

$$Z_n^{-m}(\rho,\phi) = R_n^m(\rho)\sin m\phi$$
$$Z_n^{-m}(\rho,\phi) = R_n^m(\rho)\cos m\phi$$

ϕ is the azimuthal angle with $0 \leq \phi \leq 2\pi$
ρ is the radial distance with $0 \leq \rho \leq 1$

Remember e.g. the gaussian beam:

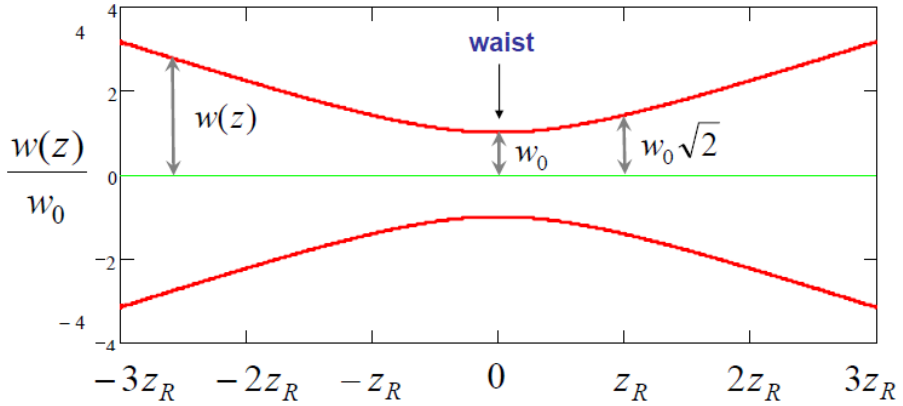

Some specific terms

$z0 = 1;$	Piston or Bias
$z1 = \rho \, \mathrm{Cos}[\theta];$	Tilt x
$z2 = \rho \, \mathrm{Sin}[\theta];$	Tilt y
$z3 = -1 + 2\rho^2;$	Power
$z4 = \rho^2 \, \mathrm{Cos}[2\theta];$	Astig x
$z5 = \rho^2 \, \mathrm{Sin}[2\theta];$	Astig y
$z6 = \rho \, (-2 + 3\rho^2) \, \mathrm{Cos}[\theta];$	Coma x
$z7 = \rho \, (-2 + 3\rho^2) \, \mathrm{Sin}[\theta];$	Coma y
$z8 = 1 - 6\rho^2 + 6\rho^4;$	Primary Spherical

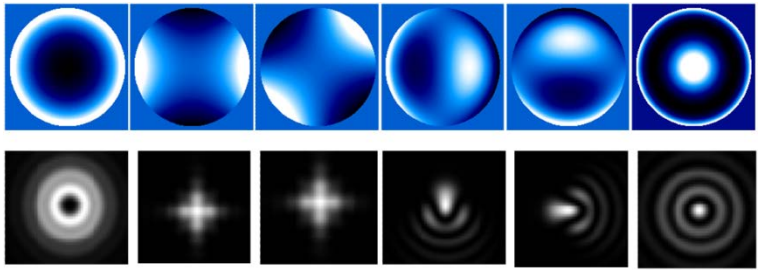

Examples of Zernike polynomials(top raw) and their corresponding far-field pattern (bottom raw). From left to right, you see defocus, 2 astigmatisms, 2 comas and spherical aberration.

Ji-Ping Zou and Benoit Wattellier (2012). „Adaptive Optics for High-Peak-Power Lasers“ in Adaptive Optics, Dr. Bob Tyson (Ed.), DOI: 10.5772/31750.

wavefront sensing: Shack Hartman Wavefront Sensor

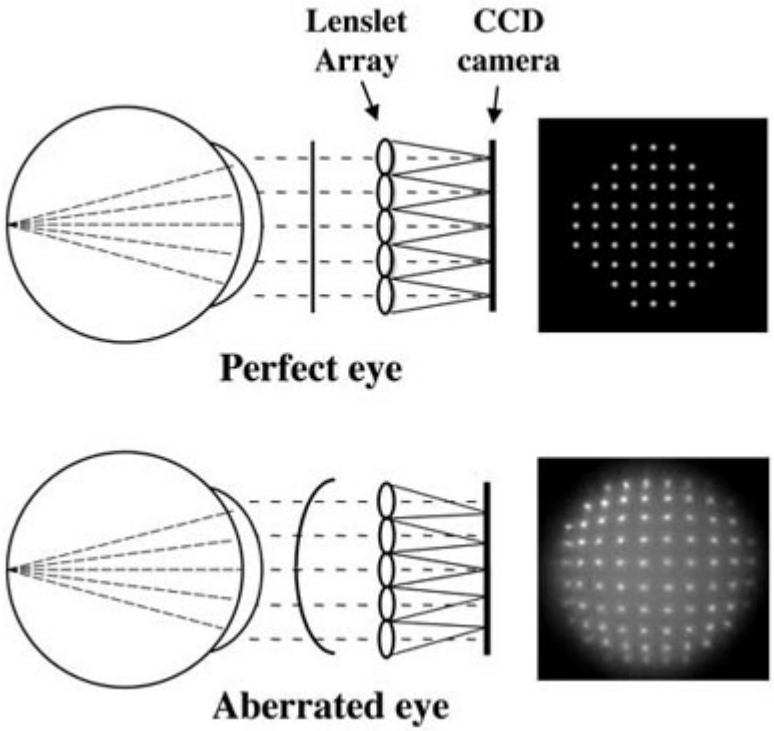

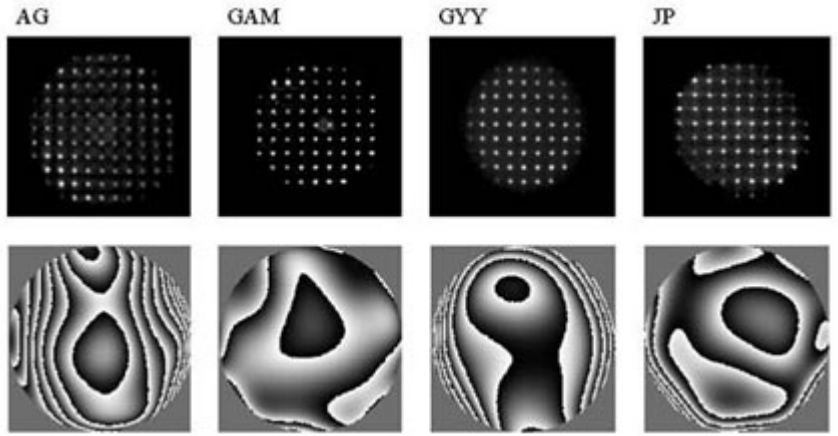

http://www.cvs.rochester.edu/williamslab/r_shackhartmann.html

Shack Hartmann LIVE

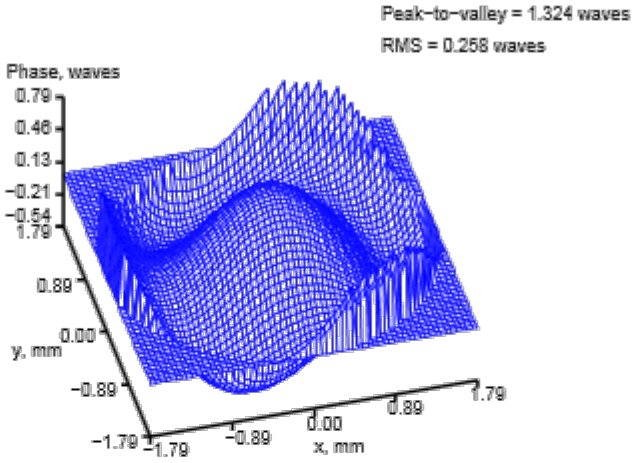

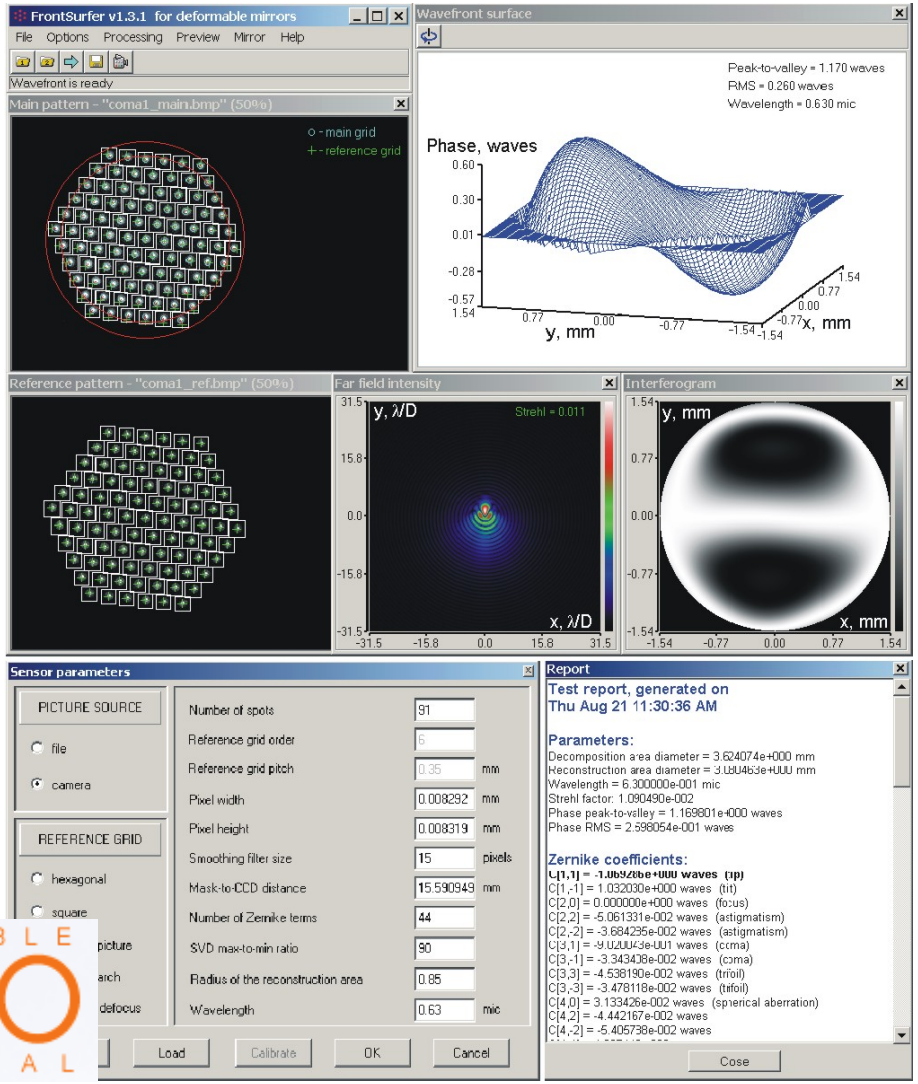

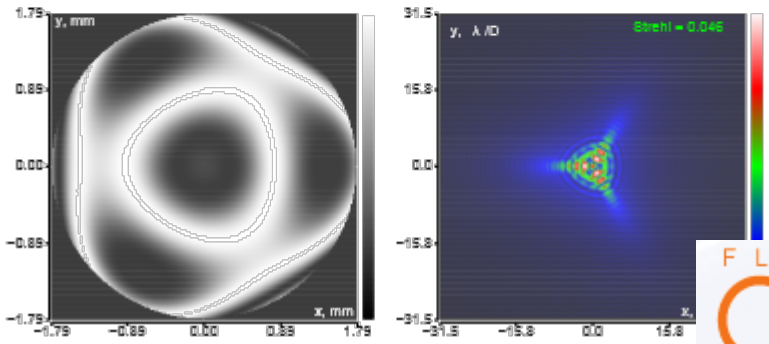

FLEXIBLE OKO OPTICAL

Zernike Modes LIVE!

FLEXIBLE OKO OPTICAL

Direct control of Zernike modes using piezo and membrane DM

Direct control of Zernike modes is beneficial in feedforward control algorithms, and in optimization-based adaptive optics, such as laser intracavity AO, adaptive image sharpness control, smart PSF control in microscopy, optimal imaging through turbulence with stochastic optimization, etc. In all these cases the dynamic control of Zernike modes provides for very quick quasi-optimal convergence to the maximum value of the target function.

Here we show a 15 mm 37-channel OKO Micromachined Membrane Deformable Mirror (MMDM) and 30 mm 37-channel Piezoelectric Deformable Mirror (PDM) operated by Zernike polynomials in feedforward control mode. *No wavefront sensor* is used during the mirror operation. Both mirrors are controlled by our free MiZer software.

http://www.youtube.com/watch?v=Rysr6yOcAEQ&feature=player_embedded

If the orthonormal set of Zernike is used, the Zernike representation leads quickly to the wave front RMS, by the formula:

$$\sigma^2 = \sum_{m,n} Z_{mn}^2$$

http://wyant.optics.arizona.edu/zernikes/zernikes.htm

X-ray Optics

Refractive from the IR to the x-ray region of the electromagnetic spectrum

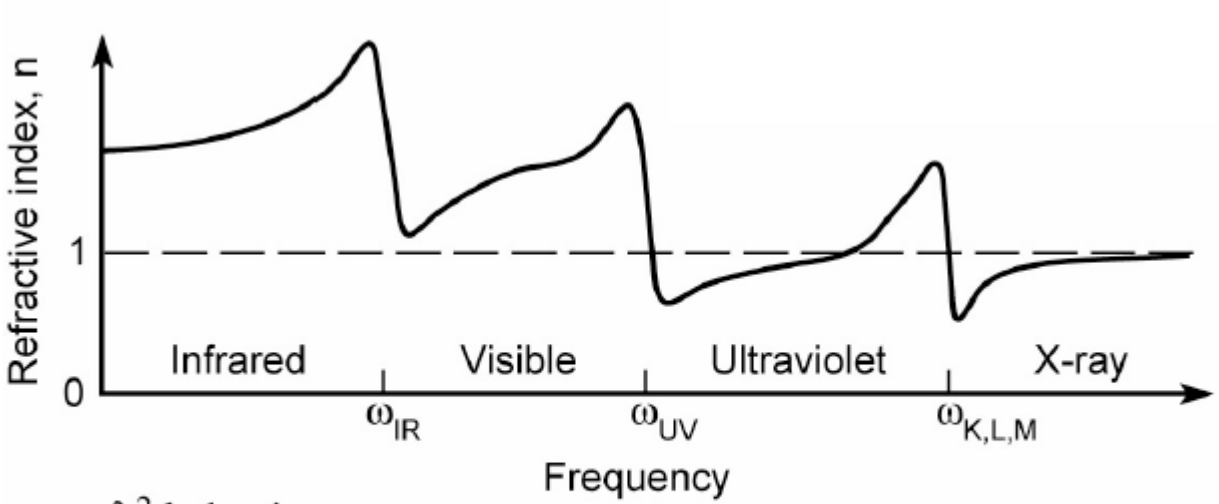

- λ^2 behavior
- δ & $\beta << 1$
- δ-crossover

Attwood, D.; Soft X-Ray and Extreme Ultraviolett Radiation, Cambridge University Press, 1999

Reflection and refraction of EUV/soft x-ray radiation

The refractive index, $n(\omega)$, is complex because EUV/soft x-ray radiation is absorbed appreciably by all atoms. This is reflected in the semi-classical model

$$n(\omega) = 1 - \frac{1}{2}\frac{e^2 n_a}{\epsilon_0 m}\sum_s \frac{g_s}{\left(\omega^2 - \omega_s^2\right) + i\gamma\omega}$$

where again $\sum_s g_s = Z$ (2.73), or by its quantum mechanical equivalent $\sum_{k,n} g_{kn} = Z$.

The convention is to express scattering and refractive index in terms of a complex scattering factor, $f^0(\omega)$ specific to each element

$$f^0(\omega) = f_1^0(\omega) - i f_2^0(\omega) = \sum_s \frac{g_s \omega^2}{\omega^2 - \omega_s^2 + i\gamma\omega}$$

where the scattering factor arises from consideration of the scattered electric field due to an atom, relative to that of a free electron, a topic we will discuss again in a later lecture. Introducing the classical electron radius

$$r_e = \frac{e^2}{4\pi\epsilon_0 m c^2}$$

The refractive index can be written as

$$n(\omega) = 1 - \frac{n_a r_e \lambda^2}{2\pi}\left[f_1^0(\omega) - i f_2^0(\omega)\right]$$

or in simpler notation

Attwood, D.; Soft X-Ray and Extreme Ultraviolett Radiation, Cambridge University Press, 1999

Refractive Index from the IR to X-ray Spectral Region

$$\tilde{n} = 1 - \delta + i\beta = 1 - \frac{r_0 \lambda^2}{2\pi} n_a (f_1^0 - i f_2^0)$$

δ	deviation of the refractive index from one
β	absorption index
f_1^0, f_2^0	real and imaginary part of the atomic scattering factor
n_a	number of atoms per volume
r_0	classical electron radius

Phase shift relative to vacuum propagation

For a wave propagating in a medium of refractive index $n = 1 - \delta + i\beta$

$$\mathbf{E}(\mathbf{r}, t) = \underbrace{\mathbf{E}_0 e^{-i\omega(t-r/c)}}_{\text{vacuum propagation}} \underbrace{e^{-i(2\pi\delta/\lambda)r}}_{\phi\text{-shift}} \underbrace{e^{-(2\pi\beta/\lambda)r}}_{\text{decay}}$$

the phase shift $\Delta\phi$ relative to vacuum, due to propagation through a thickness Δr is

$$\Delta\phi = \left(\frac{2\pi\delta}{\lambda}\right)\Delta r$$

- Flat mirrors at short wavelengths
- Transmissive, flat beamsplitters
- Bonse and Hart interferometer
- Diffractive optics for SXR/EUV

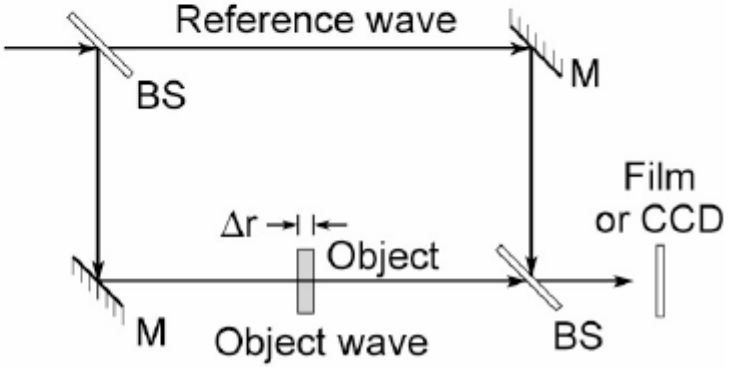

Attwood, D.; Soft X-Ray and Extreme Ultraviolett Radiation, Cambridge University Press, 1999

Spatial continuity along the interface

Continuity of parallel field components requires

$$(\mathbf{k}\cdot\mathbf{x}_0 = \mathbf{k}'\cdot\mathbf{x}_0 = \mathbf{k}_0''\cdot\mathbf{x}_0) \quad \text{at } z = 0$$

$$k_x = k_x' = k_x''$$

$$k\sin\phi = k'\sin\phi' = k''\sin\phi''$$

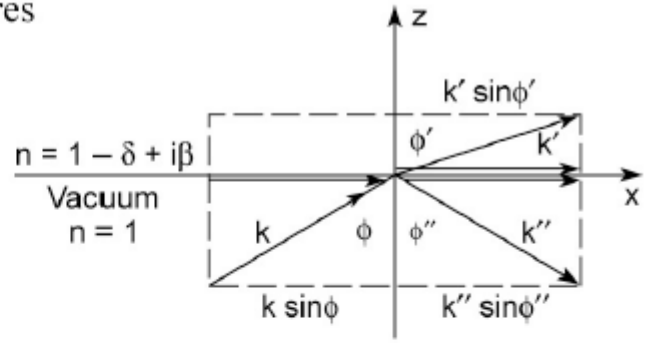

Conclusions:

Since k = k″ (both in vacuum)

$$\sin\phi = \sin\phi''$$

$$\therefore \quad \boxed{\phi = \phi''}$$

The angle of incidence equals the angle of reflection

$$k\sin\phi = k'\sin\phi' \qquad (3.36)$$

$$k = \frac{\omega}{c} \text{ and } k' = \frac{\omega'}{c/n} = \frac{n\omega}{c}$$

$$\sin\phi = n\sin\phi'$$

$$\boxed{\sin\phi' = \frac{\sin\phi}{n}}$$

Snell's Law, which describes refractive turning, for complex n.

Attwood, D.; Soft X-Ray and Extreme Ultraviolett Radiation, Cambridge University Press, 1999

Total external reflection of soft x-ray and EUV radiation

Snell's law for a refractive index of $n \simeq 1 - \delta$, assuming that $\beta \to 0$

$$\sin\phi' = \frac{\sin\phi}{1-\delta}$$

Consider the limit when $\phi' \to \frac{\pi}{2}$

$$1 = \frac{\sin\phi_c}{1-\delta}$$

$$\sin\phi_c = 1 - \delta$$

$$\sin(90^\circ - \theta_c) = 1 - \delta$$

$$\cos\theta_c = 1 - \delta$$

$$1 - \frac{\theta_c^2}{2} + \cdots = 1 - \delta$$

$$\boxed{\theta_c = \sqrt{2\delta}}$$

The critical angle for total external reflection.

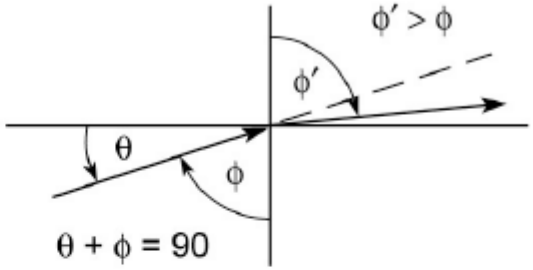

Glancing incidence ($\theta < \theta_c$) and total external reflection

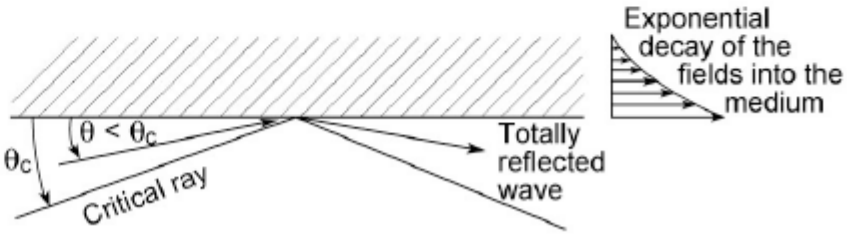

Attwood, D.; Soft X-Ray and Extreme Ultraviolett Radiation, Cambridge University Press, 1999

Total external reflection

$$\boxed{\theta_c = \sqrt{2\delta}}$$

$$\delta = \frac{n_a r_e \lambda^2 f_1^0(\lambda)}{2\pi}$$

$$\theta_c = \sqrt{2\delta} = \sqrt{\frac{n_a r_e \lambda^2 f_1^0(\lambda)}{\pi}}$$

The atomic density n_a, varies slowly among the natural elements, thus to first order

$$\theta_c \propto \lambda\sqrt{Z}$$

where f_1^0 is approximated by Z. Note that f_1^0 is a complicated function of wavelength (photon energy) for each element.

Attwood, D.; Soft X-Ray and Extreme Ultraviolett Radiation, Cambridge University Press, 1999

Galcing incidence reflection (s-polarization)

$$R_s = \frac{\left|\cos\phi - \sqrt{n^2 - \sin^2\phi}\right|^2}{\left|\cos\phi + \sqrt{n^2 - \sin^2\phi}\right|^2}$$

For $\theta = 90^\circ - \phi \le \theta_c$

where $\theta_c = \sqrt{2\delta} \ll 1$

$$\cos\phi = \sin\theta \simeq \theta$$

$$\sin^2\phi = 1 - \cos^2\phi = 1 - \sin^2\theta \simeq 1 - \theta^2$$

For $n = 1 - \delta + i\beta$

$$n^2 = (1-\delta)^2 + 2i\beta(1-\delta) - \beta^2$$

$$R_{s,\theta} = \frac{\left|\theta - \sqrt{(\theta^2 - \theta_c^2) + 2i\beta}\right|^2}{\left|\theta + \sqrt{(\theta^2 - \theta_c^2) + 2i\beta}\right|^2} \qquad (\theta \ll 1)$$

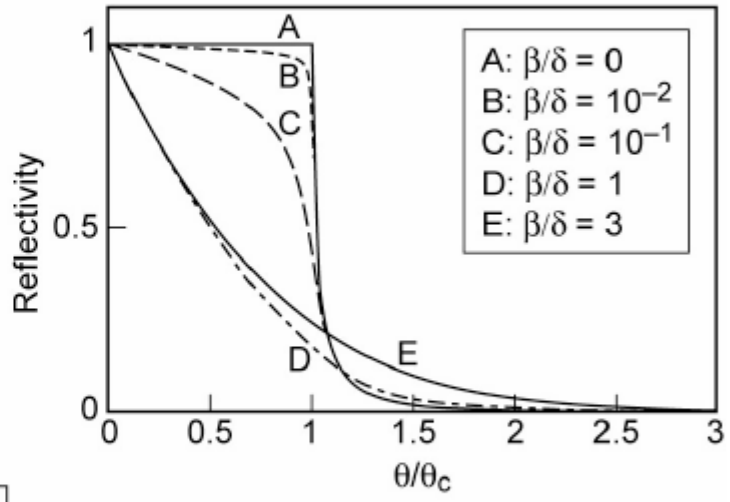

E. Nähring, "Die Totalreflexion der Röntgenstrahlen", Physik. Zeitstr. XXXI, 799 (Sept. 1930).

Attwood, D.; Soft X-Ray and Extreme Ultraviolett Radiation, Cambridge University Press, 1999

The „attosecond filter“

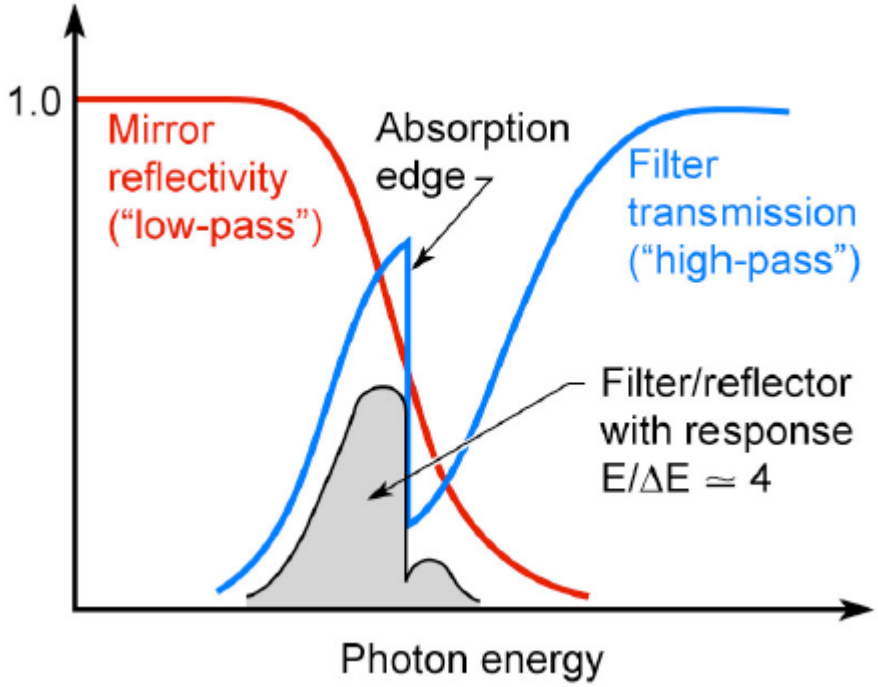

- Combines a glacing incidence mirror and a filter
- Modest resolution $E/\Delta E$ = 3-5
- Commonly used

Determining f_1^2 and f_2^0

- f_2^0 easily measured by absorption
- f_1^0 difficult in SXR/EUV region
- Common to use Kramers-Kronig relations

$$f_1^0(\omega) = Z - \frac{2}{\pi}\mathcal{P}_C \int_0^\infty \frac{u f_2^0(u)}{u^2 - \omega^2}\, du$$

$$f_2^0 = \frac{2\omega}{\pi}\mathcal{P}_C \int_0^\infty \frac{f_1^0(u) - Z}{u^2 - \omega^2}\, du$$

as in the Henke & Gullikson tables

- Possible to use reflection from clean surfaces; Soufli & Gullikson
- With diffractive beam splitter can use a phase-shifting interferometer; Chang et al.
- Bi-mirror technique of Joyeux, Polack and Phalippou (Orsay, France)

Attwood, D.; Soft X-Ray and Extreme Ultraviolett Radiation, Cambridge University Press, 1999

Is there a „Brewster“ angle in the x-ray and EUV?

For p-polarization

$$R_p = \left|\frac{E_0''}{E_0}\right|^2 = \frac{\left|n^2\cos\phi - \sqrt{n^2 - \sin^2\phi}\right|^2}{\left|n^2\cos\phi + \sqrt{n^2 - \sin^2\phi}\right|^2} \qquad (3.56)$$

There is a minimum in the reflectivity where the numerator satisfies

$$n^2\cos\phi_B = \sqrt{n^2 - \sin^2\phi_B} \qquad (3.58)$$

Squaring both sides, collecting like terms involving ϕ_B, and factoring, one has

$$n^2(n^2 - 1) = (n^4 - 1)\sin^2\phi_B$$

or

$$\sin\phi_B = \frac{n}{\sqrt{n^2 + 1}}$$

the condition for a minimum in the reflectivity, for parallel polarized radiation, occurs at an angle given by

$$\tan\phi_B = n \qquad (3.59)$$

For complex n, Brewster's minimum occurs at

$$\tan\phi_B = 1 - \delta$$

or

$$\boxed{\phi_B \simeq \frac{\pi}{4} - \frac{\delta}{2}} \qquad (3.60)$$

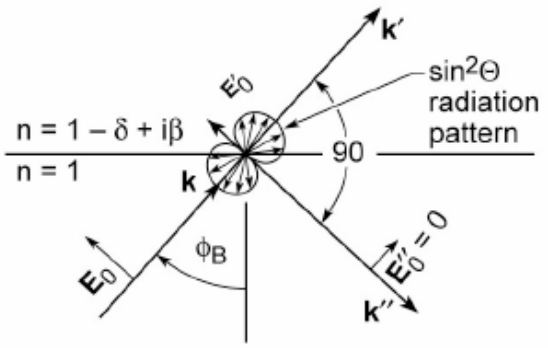

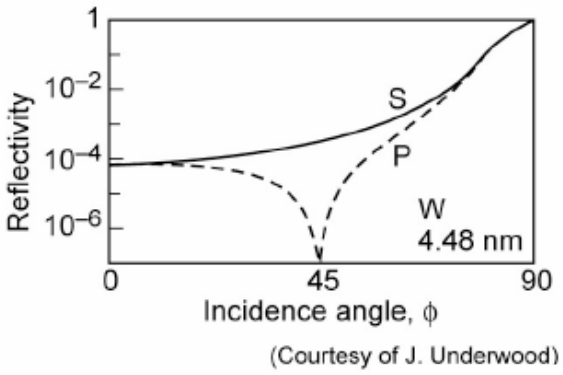

(Courtesy of J. Underwood)

Attwood, D.; Soft X-Ray and Extreme Ultraviolett Radiation, Cambridge University Press, 1999

grazing incidence optics

Ellipse: p + q = constant, $\theta_{in} = \theta_{out}$
Focusing: equivalent optical path lengths from source-to-focus
'Ideal' mirror would have an elliptical (2D) or ellipsoidal (3D) surface figure

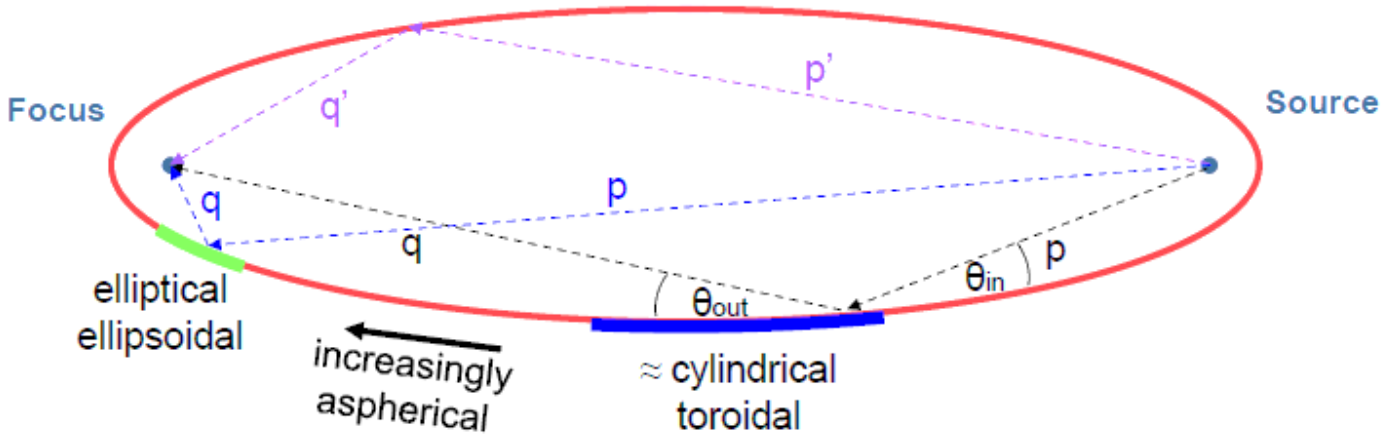

focus size ≈ source size x q/p

Micro/nanofocusing applications:

- good ellipsoidal mirrors not readily manufacturable
- perpendicular elliptical mirrors
  - Kirkpatrick-Baez (KB) configuration

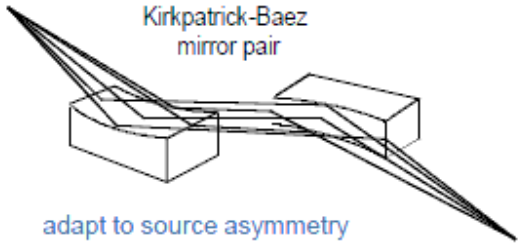

adapt to source asymmetry
- apertures
- demagnification

P. Kirkpatrick, A. V. Baez, Journal Opt. Soc. Am., vol. 38, pp. 766-774, 1948

Wolter optics Type I

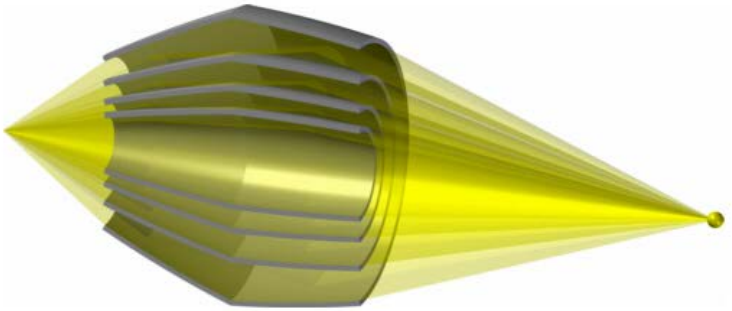

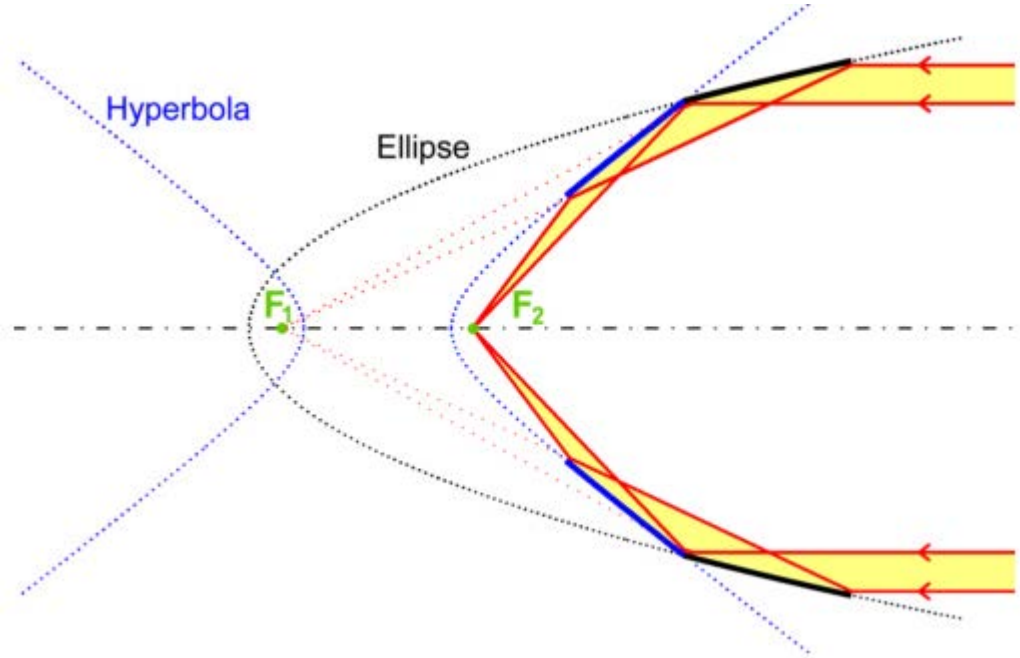

DOI: 10.1002/andp.19524450108

Wolter Optics – Type II

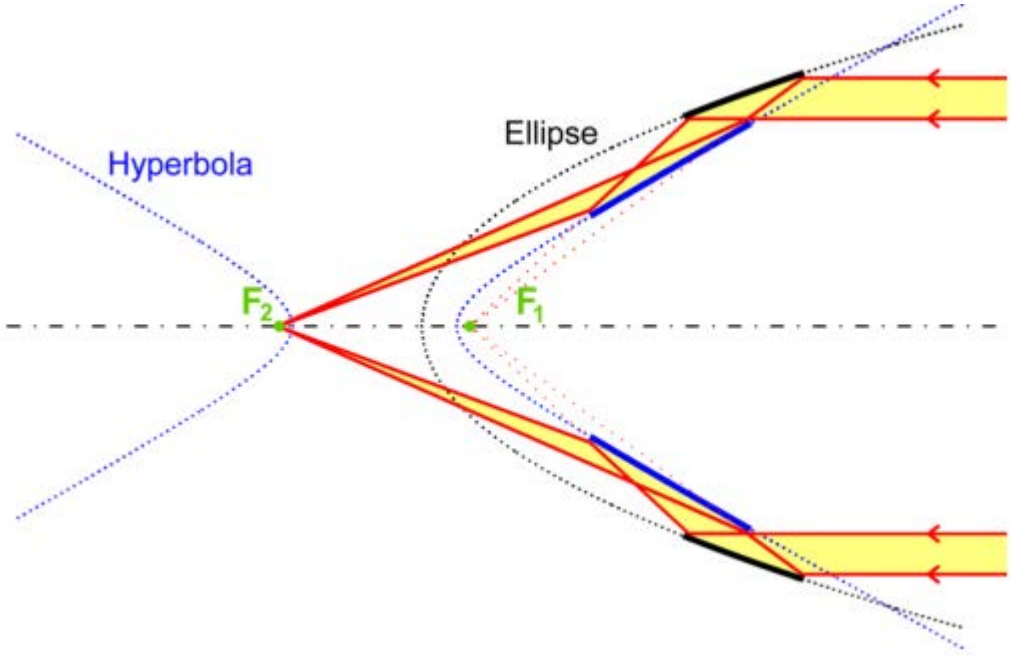

DOI: 10.1002/andp.19524450108

Wolter Optics – Type III

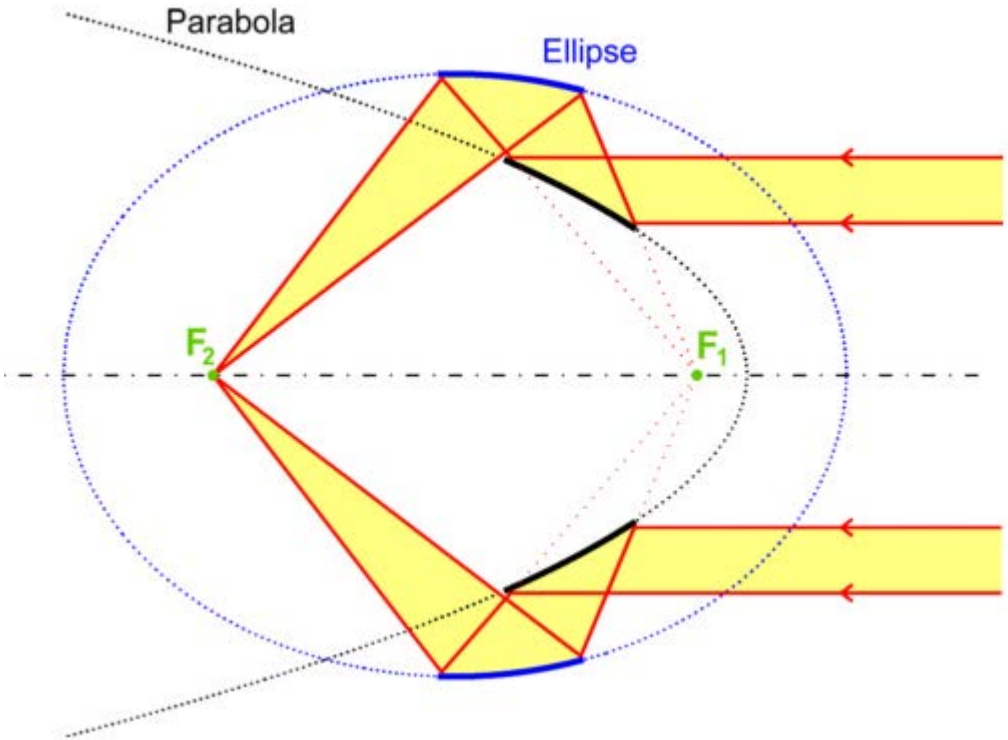

DOI: 10.1002/andp.19524450108

Schwarzschild optics

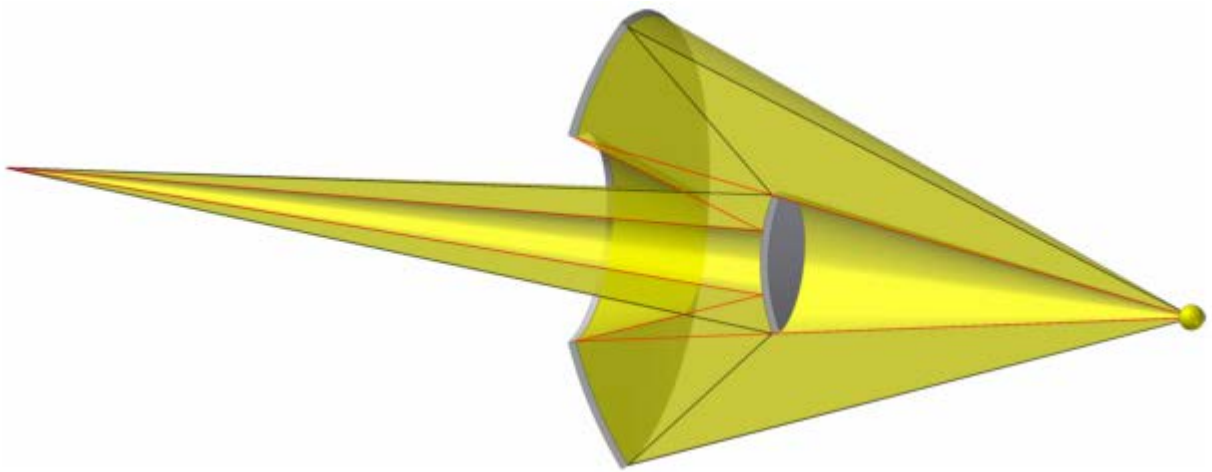

K. Schwarzschild, Untersuchungen zur geometrischen Optik, II. Astronomische Mitteilungen der Königlichen Sternwarte zu Göttingen, vol. 10, pp. 4-28, 1905

Zone plates

Zone Plate Lens

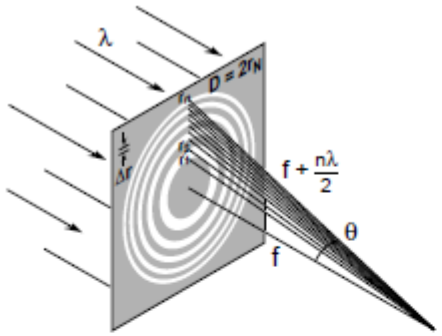

Soft X-Ray Microscope

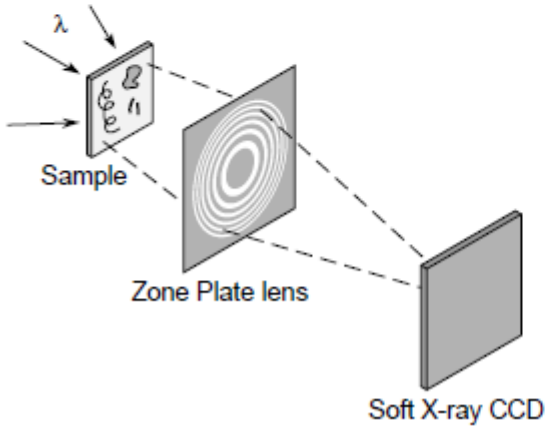

Zone Plate Formulae

$r_n^2 = n\lambda f + \frac{n^2\lambda^2}{4}$	(9.9)	$\lambda = 2.5$ nm, $\Delta r = 25$ nm, $N = 618$
$D = 4N\Delta r$	(9.13)	63 µm
$f = \frac{4N(\Delta r)^2}{\lambda}$	(9.14)	0.63 mm
$NA = \frac{\lambda}{2\Delta r}$	(9.15)	0.05 µm
$\text{Res.} = k_1 \frac{\lambda}{\text{NA}} = 2k_1\Delta r$	$k_1 = 0.61$ ($\sigma = 0$)	$1.22\Delta r = 30$ nm
	$k_1 = 0.4$ ($\sigma = 0.45$)	$0.8\Delta r = 19$ nm
$\text{DOF} = \pm\frac{1}{2}\frac{\lambda}{(\text{NA})^2}$	(9.50)	1 µm
$\frac{\Delta\lambda}{\lambda} \le \frac{1}{N}$	(9.52)	1/700

Professor David Attwood
Univ. California, Berkeley

Zone plates II

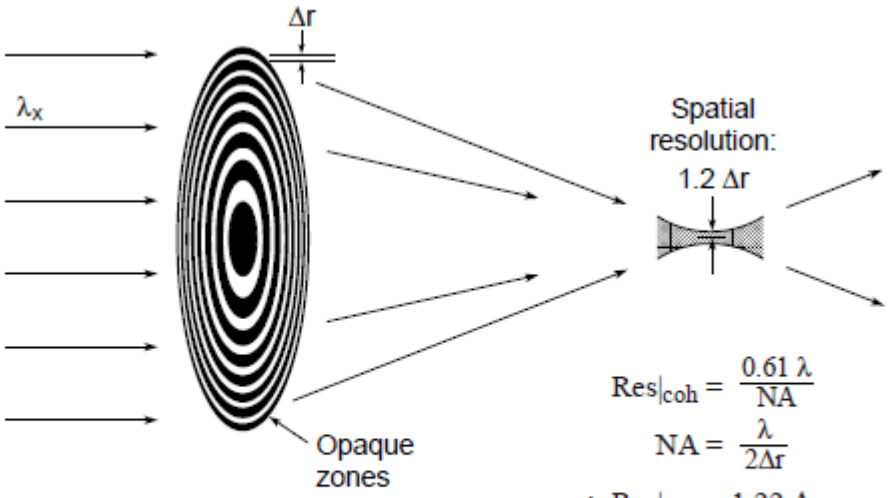

$$\mathrm{Res}|_{coh} = \frac{0.61\,\lambda}{NA}$$

$$NA = \frac{\lambda}{2\Delta r}$$

$$\therefore \mathrm{Res}|_{coh} = 1.22\,\Delta r$$

(σ = 0, see first slide)

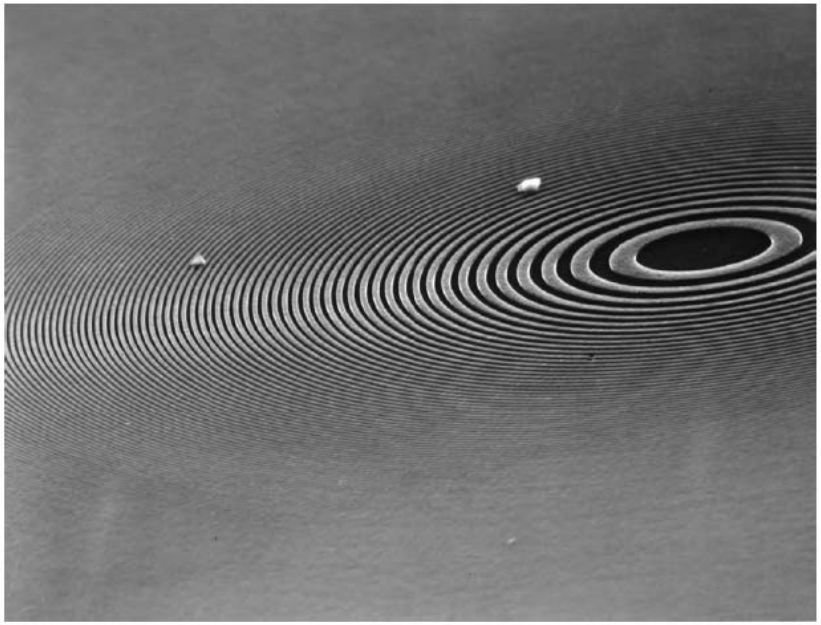

E. Anderson, LBNL

Attwood, D.; Soft X-Ray and Extreme Ultraviolett Radiation, Cambridge University Press, 1999

Zone Plate III

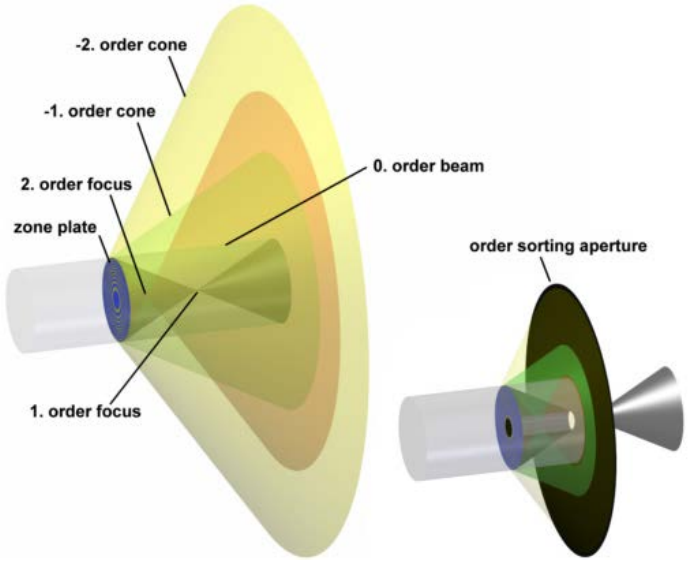

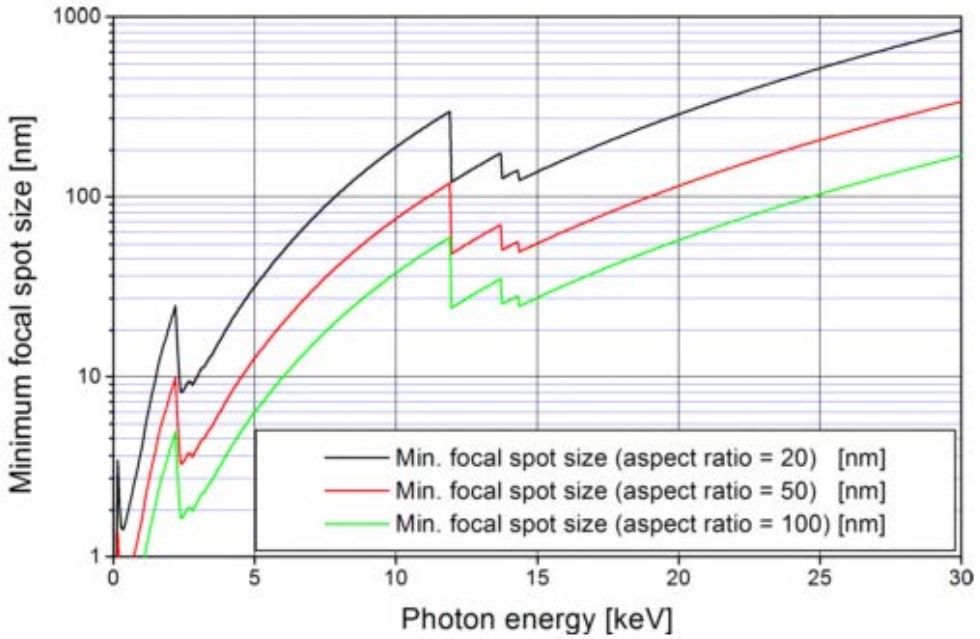

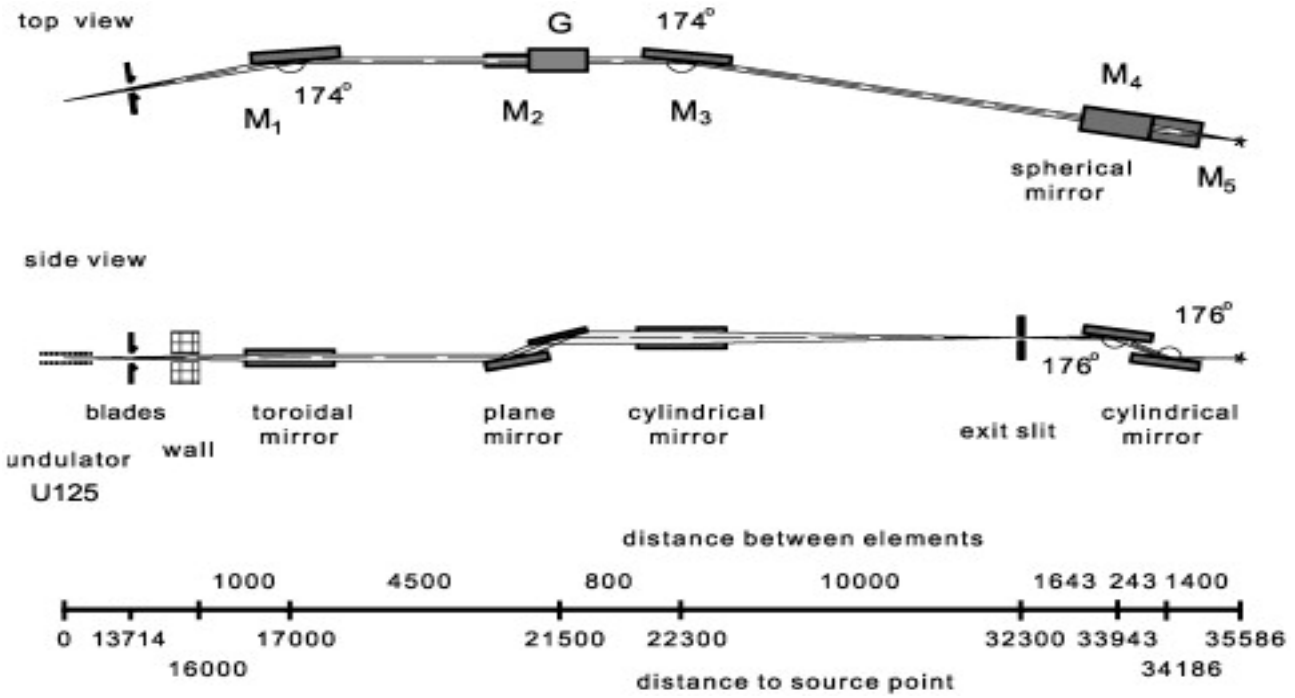

Fig. 1 Optical design of the U125/1-PGM. This monochromator was the first collimated PGM installed at BESSY II.

The versatility of collimated plane grating monochromators

Nuclear Instruments and Methods in Physics Research Section A: Accelerators, Spectrometers, Detectors and Associated Equipment Volumes 467/468, Part 1 2001 418 - 425
http://dx.doi.org/10.1016/S0168-9002(01)00338-2

dynamic adaption to optimise focus/wavefront

major classes:

- piezoelectric bimorph systems
- mechanically actuated systems
- Extension of these technologies
  - Increased number of actuators to correct local figure errors
  - Active optics (adaptive optics)

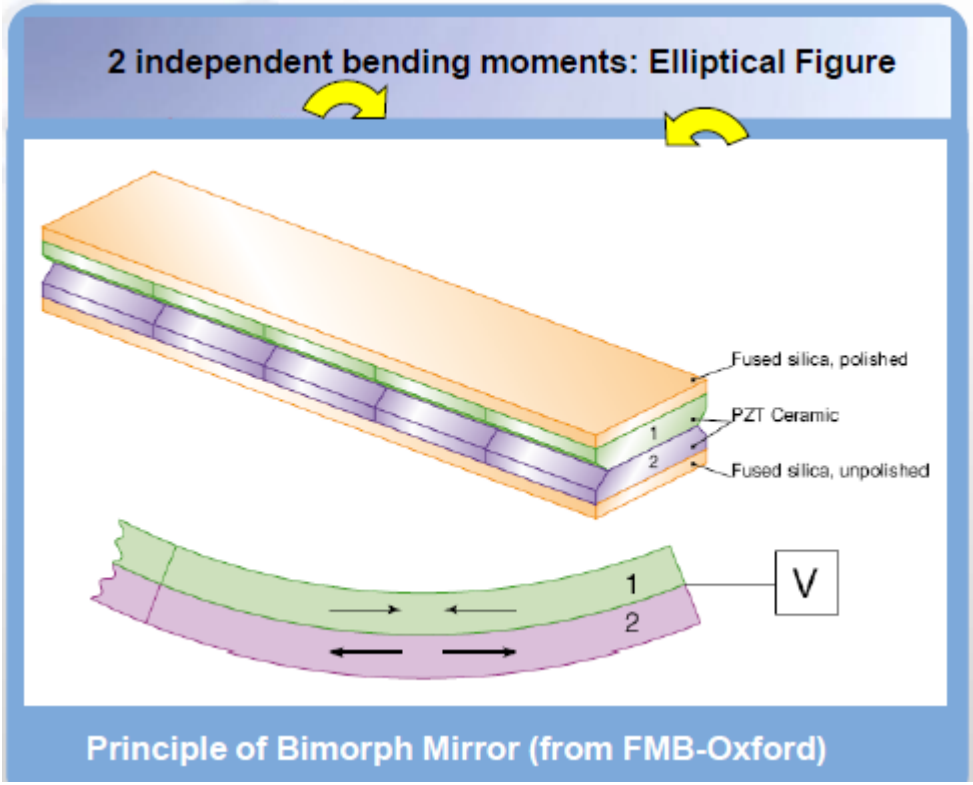

Multilayer Interference Coatings

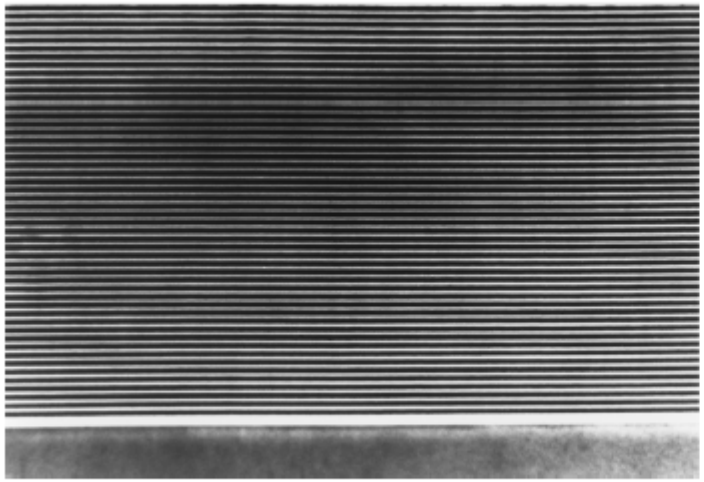

(W/C, T. Nguyen)

$$m\lambda = 2d \sin\theta$$

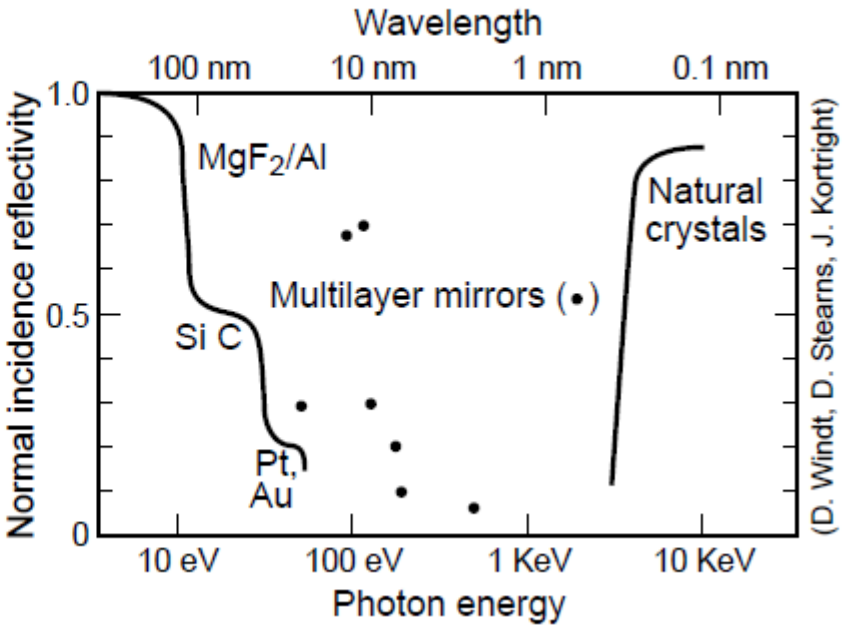

Attwood, D.; Soft X-Ray and Extreme Ultraviolett Radiation, Cambridge University Press, 1999

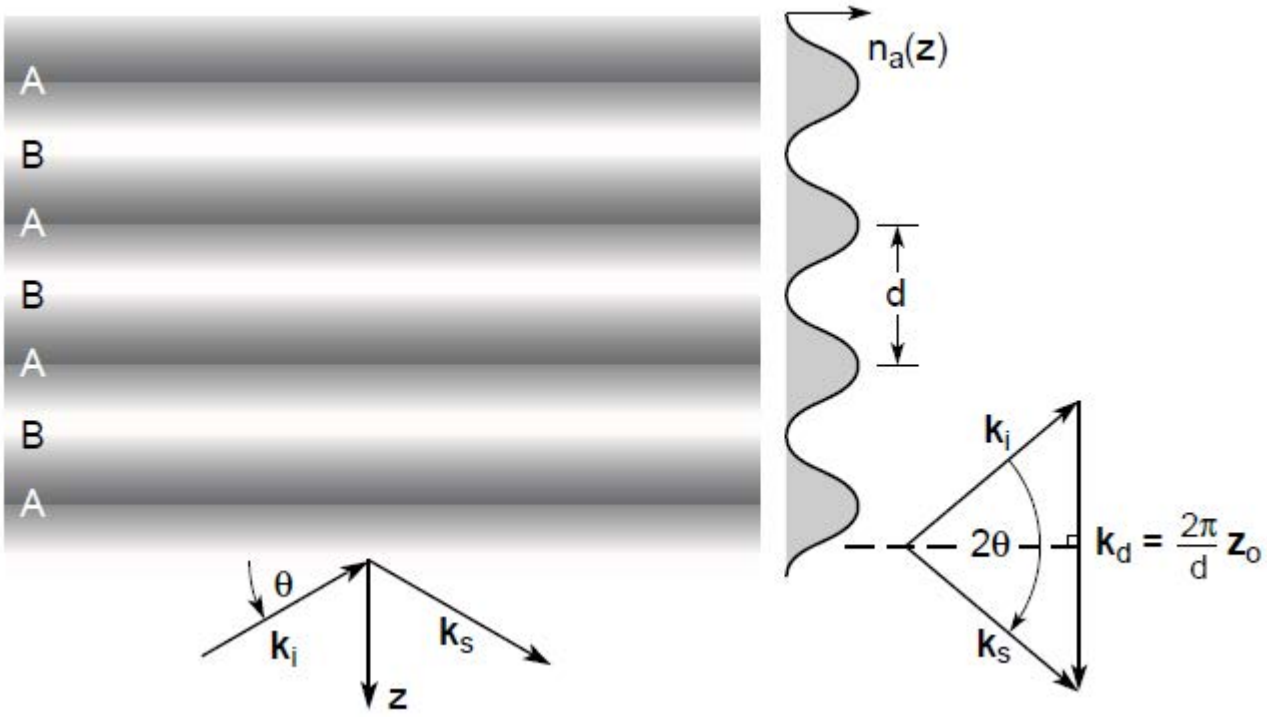

Attwood, D.; Soft X-Ray and Extreme Ultraviolett Radiation, Cambridge University Press, 1999

High Refelectivity Mirror Coatings Require

- Refractive index contrast at the interfaces
- Minimal Absorption in the low-Z material
- Thin high-Z layer where possible $\Gamma \equiv \Delta\tau_H/(\Delta\tau_H + \Delta\tau_L)$
- Interfaces wich are chemically stable with time
- Minimal interdiffusion at the interfaces
- Minimal interfacial roughness (no crystallite formation with the layers, no shadowing in the coating process, surface mobility)
- Thermal stability during illumination
- Chemically stable vacuum interface (e. g. capping layer)
- Uniform coating thickness

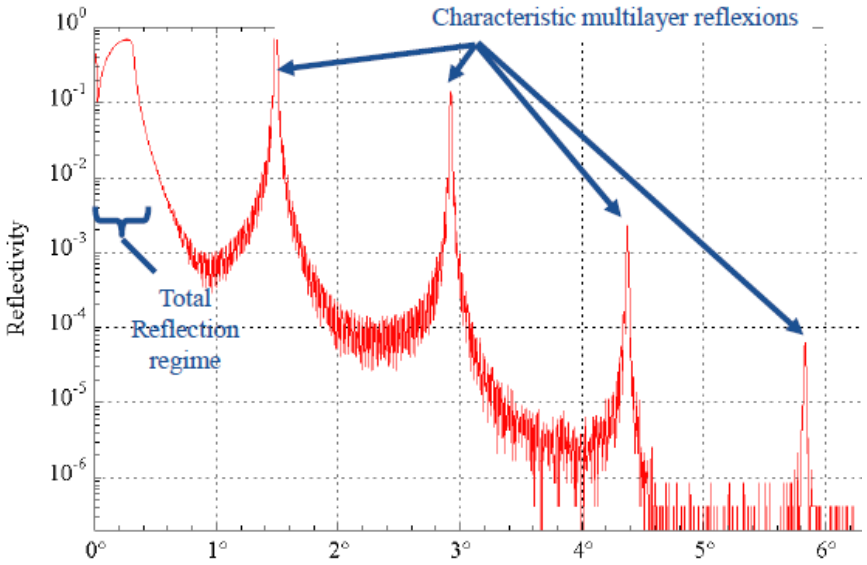

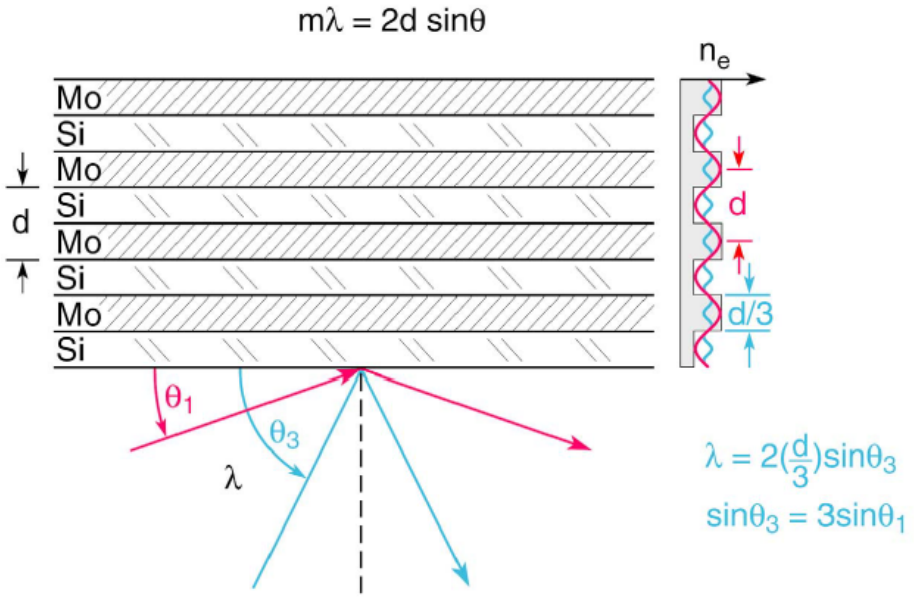

an angular scan of a multilayer mirror performs a fourier-transform of the density profile

Multilayer Interface Mirrors Computational Modelling

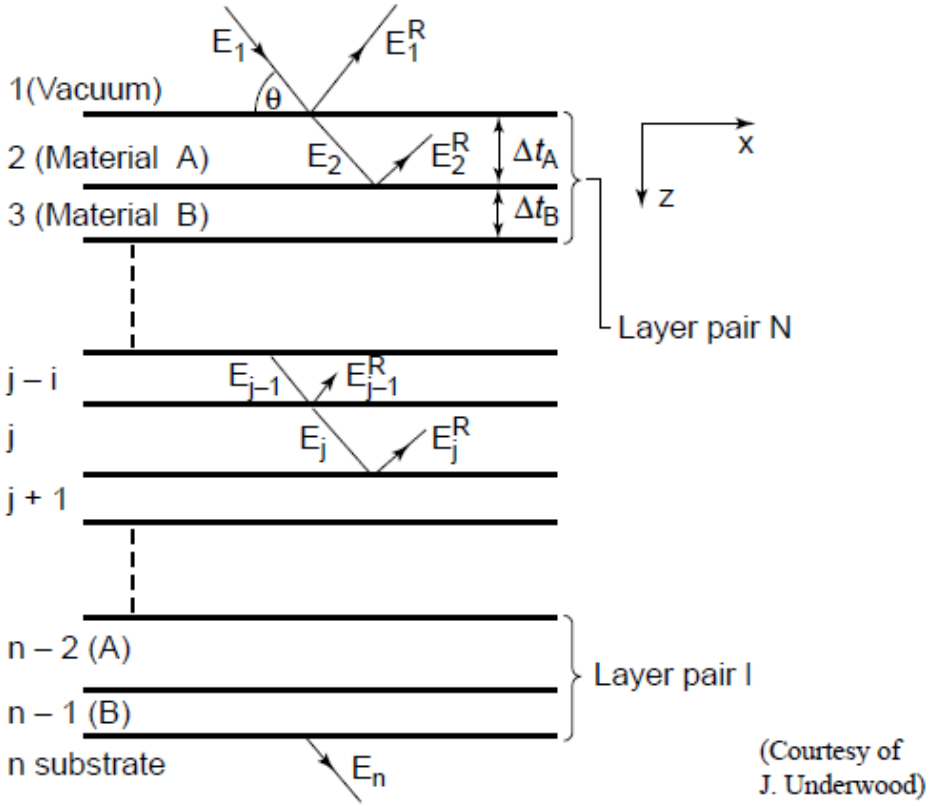

(Courtesy of J. Underwood)

With refractive index n:

$$n = 1 - \delta + i\beta = 1 - \frac{n_a r_e \lambda^2}{2\pi}(f_1^0 - if_2^0)$$

Fresnel equations

s-polarized light

$$R_\mathrm{s} = \left| \frac{n_1 \cos\theta_\mathrm{i} - n_2 \cos\theta_\mathrm{t}}{n_1 \cos\theta_\mathrm{i} + n_2 \cos\theta_\mathrm{t}} \right|^2 = \left| \frac{n_1 \cos\theta_\mathrm{i} - n_2 \sqrt{1 - \left(\frac{n_1}{n_2} \sin\theta_\mathrm{i}\right)^2}}{n_1 \cos\theta_\mathrm{i} + n_2 \sqrt{1 - \left(\frac{n_1}{n_2} \sin\theta_\mathrm{i}\right)^2}} \right|^2$$

p-polarized light

$$R_\mathrm{p} = \left| \frac{n_1 \cos\theta_\mathrm{t} - n_2 \cos\theta_\mathrm{i}}{n_1 \cos\theta_\mathrm{t} + n_2 \cos\theta_\mathrm{i}} \right|^2 = \left| \frac{n_1 \sqrt{1 - \left(\frac{n_1}{n_2} \sin\theta_\mathrm{i}\right)^2} - n_2 \cos\theta_\mathrm{i}}{n_1 \sqrt{1 - \left(\frac{n_1}{n_2} \sin\theta_\mathrm{i}\right)^2} + n_2 \cos\theta_\mathrm{i}} \right|^2$$

Example

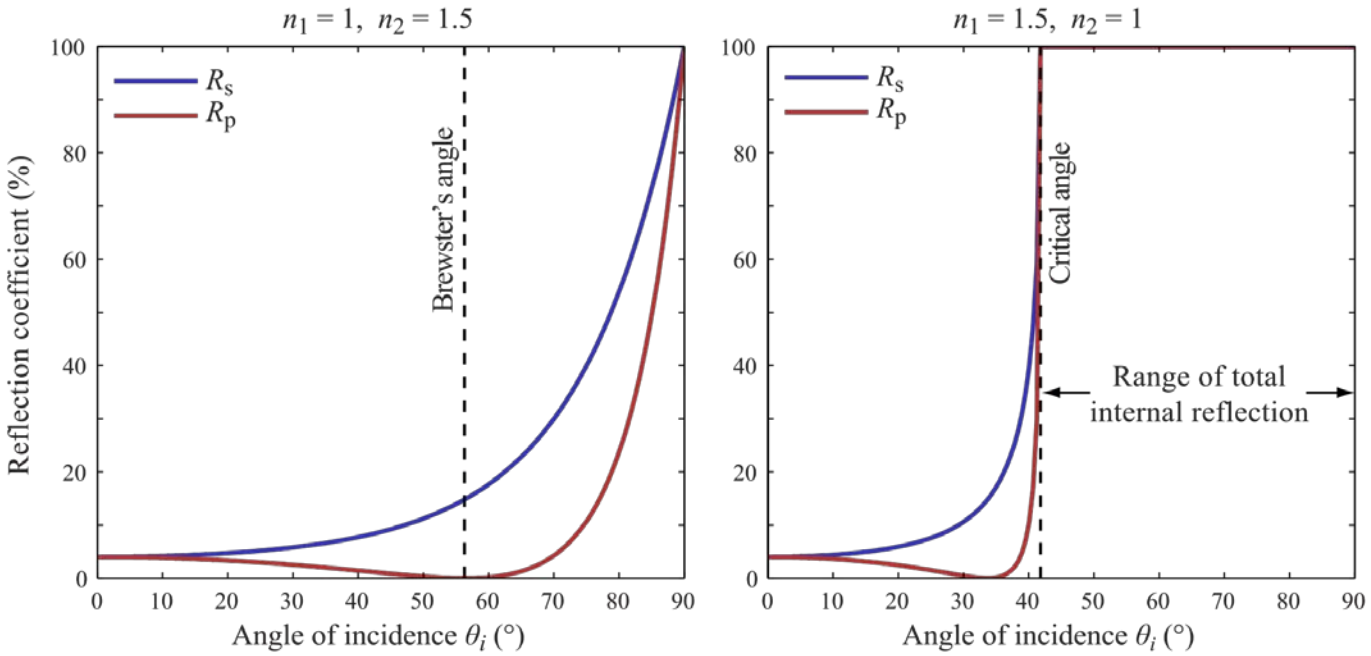
$n_1 = 1,\ n_2 = 1.5$
R_s
R_p
Brewster's angle
Reflection coefficient (%)
Angle of incidence θ_i (°)
$n_1 = 1.5,\ n_2 = 1$
R_s
R_p
Critical angle
Range of total internal reflection
Angle of incidence θ_i (°)

Methods to simulate multilayer mirrors

- Transfer Matrix Method
  - Abeles matrix formalism
- recursive Rouard method

simulation resources

http://www.rxollc.com/idl/

http://henke.lbl.gov/optical_constants/

Boundary Conditions at interfaces

The boundary conditions require that the electric and magnetic fields be continous at each interface. This can be expressed as follows:

first interface	second interface
$n_0 E_0 - n_0 E_0' = n_1 E_1 - n_1 E_1'$	$n_1 E_1 \cdot e^{ikl} - n_1 E_1' \cdot e^{-ikl} = n_T E_T$

where l is the length of the medium

In matrix form this can be expressed as

$$\begin{bmatrix} 1 \\ n_0 \end{bmatrix} + \begin{bmatrix} 1 \\ -n_0 \end{bmatrix} \frac{E_0'}{E_0} = \begin{bmatrix} \cos kl & \frac{-i}{n_1} \sin kl \\ -i n_1 \sin kl & \cos kl \end{bmatrix} \begin{bmatrix} 1 \\ n_T \end{bmatrix} \frac{E_T}{E_0}$$

Fowles, G. A.; Introduction to modern Optics; Dover Publications, 2009

Multiple optical interfaces

Using the following abbreviations

$$r = \frac{E_0'}{E_0} \qquad t = \frac{E_T}{E_0}$$

with r the reflection coefficient and t the transmission coefficient we can write

$$\begin{bmatrix} 1 \\ n_0 \end{bmatrix} + \begin{bmatrix} 1 \\ -n_0 \end{bmatrix} r = M \begin{bmatrix} 1 \\ n_T \end{bmatrix} t$$

The matrix M is known as the *transfer matrix*

$$M = \begin{bmatrix} \cos kl & \frac{-i}{n_1} \sin kl \\ -in_1 \sin kl & \cos kl \end{bmatrix}$$

Assuming N interfaces

For a number of N layers the total transfer matrix is derived by

$$\prod_{i=1}^{N} M_i = M_1 M_2 M_3 \dots M_N = M$$

where $M = \begin{bmatrix} A & B \\ C & D \end{bmatrix}$

thus the total reflection and transmission of a system with N interfaces is written as

$$r = \frac{An_0 + Bn_0 n_T - C - Dn_T}{An_0 + Bn_T n_0 + C + Dn_T}$$

$$t = \frac{2n_0}{An_0 + Bn_T n_0 + C + Dn_T}$$

Transfer Matrix for periodic high reflectance films

Example:
quarter wavelength film of alternating layer of high and low refractive index materials

Transfer matrix for a double layer:

$$\begin{bmatrix} 0 & \frac{-i}{n_L} \\ -in_L & 0 \end{bmatrix}\begin{bmatrix} 0 & \frac{-i}{n_H} \\ -in_H & 0 \end{bmatrix} = \begin{bmatrix} \frac{-n_H}{n_L} & 0 \\ 0 & \frac{-n_L}{n_H} \end{bmatrix}$$

Transfer matrix for 2N layers:

$$M = \begin{bmatrix} \frac{-n_H}{n_L} & 0 \\ 0 & \frac{-n_L}{n_H} \end{bmatrix}^N = \begin{bmatrix} \left(\frac{-n_H}{n_L}\right)^N & 0 \\ 0 & \left(\frac{-n_L}{n_H}\right)^N \end{bmatrix}$$

Total reflectivity for a 2N layer film

Assuming $n_0 = 1$ for the first interface

$$R = |r^2| = \left[\frac{\left(-\frac{n_H}{n_L}\right)^N - \left(-\frac{n_L}{n_H}\right)^N}{\left(-\frac{n_H}{n_L}\right)^N + \left(-\frac{n_L}{n_H}\right)^N}\right]^2 = \left[\frac{\left(\frac{n_H}{n_L}\right)^{2N} - 1}{\left(\frac{n_H}{n_L}\right)^{2N} + 1}\right]^2$$

Smooth Multilayer Cotings are Required to Minimize Wavefront Errors in EUV Optical Systems

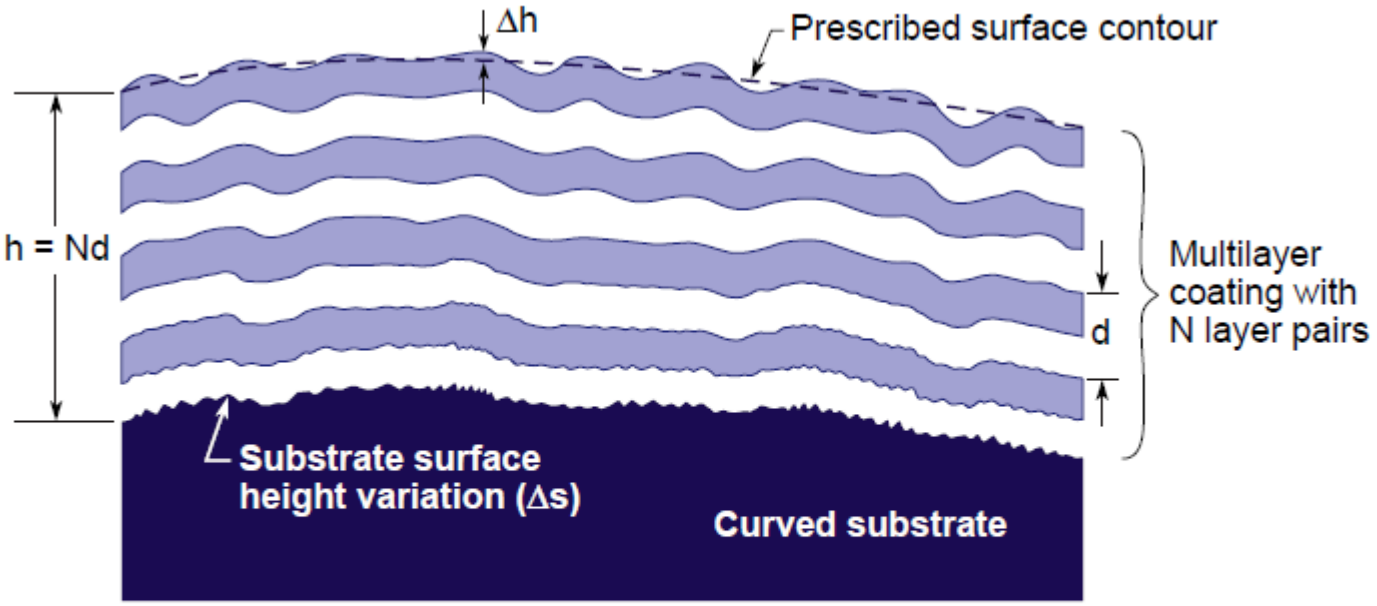

$$\Delta h = \frac{1}{2\sqrt{5}\sqrt{N_S}} \frac{\lambda}{25}$$

$$\frac{\Delta d}{d} = \frac{1}{25\sqrt{5}\sqrt{N_S}\,N}$$

- $\frac{\lambda}{25}$ total rms wavefront error
- $\Delta h_{rms} = \Delta s_{rms}/2$
- double path in reflection

Attwood, D.; Soft X-Ray and Extreme Ultraviolett Radiation, Cambridge University Press, 1999

Example: Mo/Si Multilayer

σ_a(barns/atom) = μ(cm^2/g) × 46.64
E(keV)μ(cm^2/g) = f_2^0 × 1498.22

Silicon (Si)
Z = 14
Atomic weight = 28.086

Energy (eV)	f_1^0	f_2^0	μ(cm^2/g)
30	3.799	3.734E–01	1.865E+04
70	2.448	5.701E–01	1.220E+04
100	–5.657	4.580E+00	6.862E+04
300	12.00	6.439E+00	3.216E+04
700	13.31	1.951E+00	4.175E+03
1000	13.00	1.070E+00	1.602E+03
3000	14.23	1.961E+00	9.792E+02
7000	14.33	4.240E–01	9.075E+01
10000	14.28	2.135E–01	3.199E+01
30000	14.02	2.285E–02	1.141E+00

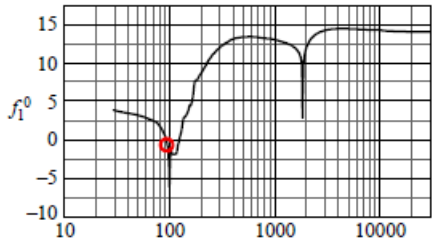

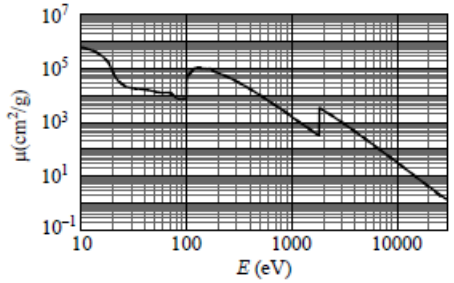

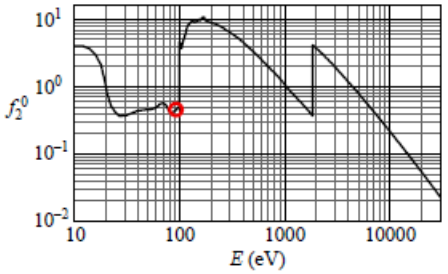

Edge Energies: K 1838.9 eV
L_1 149.7 eV
L_2 99.8 eV
L_3 99.2 eV

σ_a(barns/atom) = μ(cm^2/g) × 159.31
E(keV)μ(cm^2/g) = f_2^0 × 438.59

Molybdenum (Mo)
Z = 42
Atomic weight = 95.940

Energy (eV)	f_1^0	f_2^0	μ(cm^2/g)
30	1.071	5.292E+00	7.736E+04
70	19.38	4.732E+00	2.965E+04
100	14.02	1.124E+00	4.931E+03
300	4.609	1.568E+01	2.292E+04
700	31.41	1.819E+01	1.140E+04
1000	35.15	1.188E+01	5.210E+03
3000	35.88	1.366E+01	1.997E+03
7000	42.11	3.493E+00	2.189E+02
10000	41.67	1.881E+00	8.248E+01
30000	42.04	1.894E+00	2.769E+01

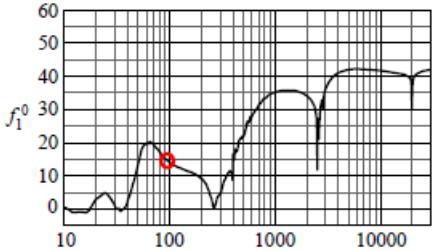

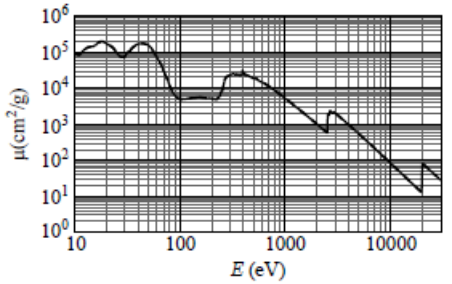

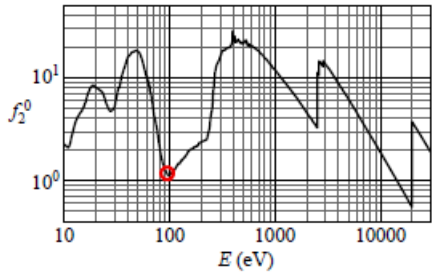

Edge Energies: K 19999.5 eV
L_1 2865.5 eV
L_2 2625.1 eV
L_3 2520.2 eV
M_1 506.3 eV
M_2 411.6 eV
M_3 394.0 eV
M_4 231.1 eV
M_5 227.9 eV
N_1 63.2 eV
N_2 37.6 eV
N_3 35.5 eV

http://henke.lbl.gov/optical_constants/

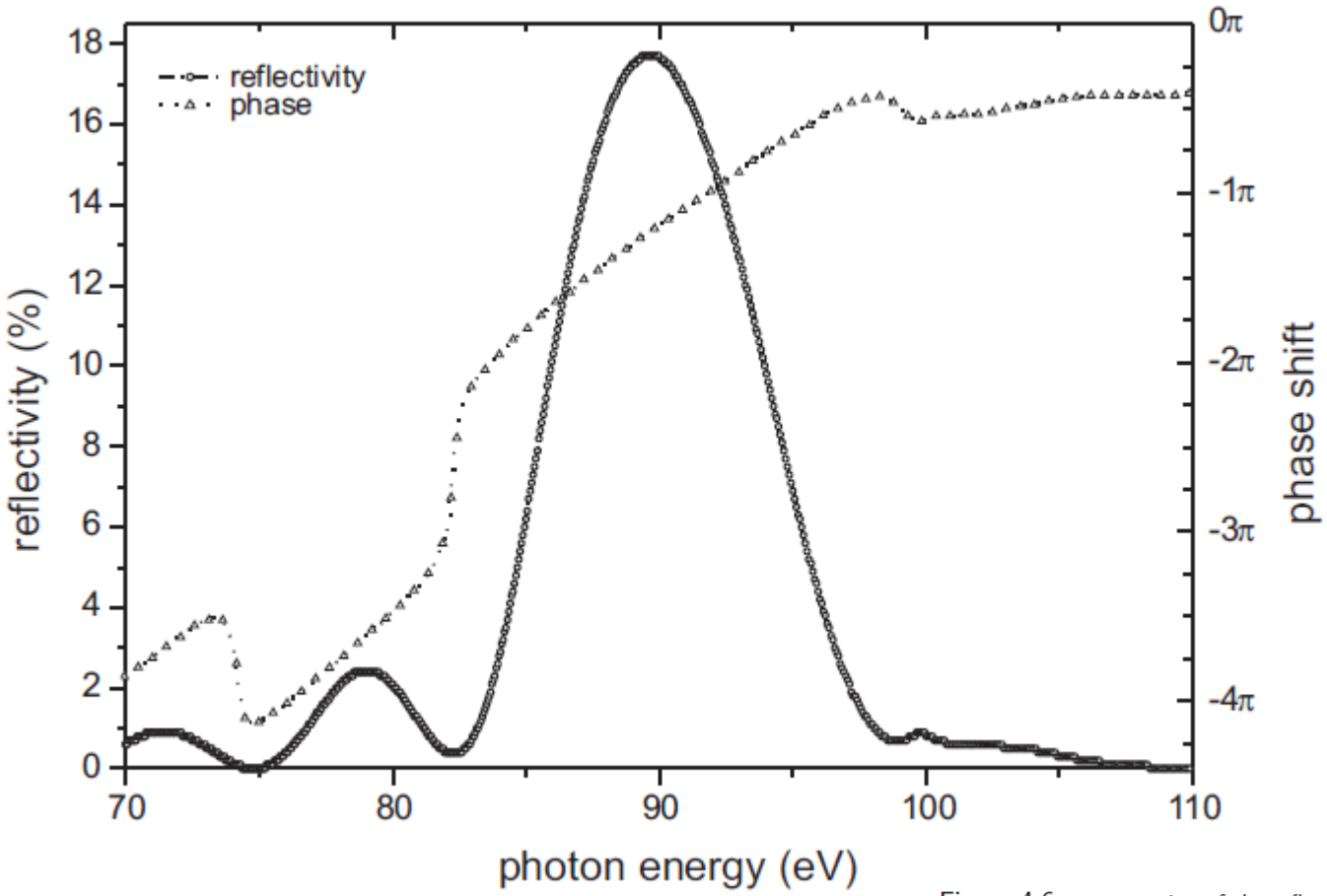

Figure 4.6: computation of the reflectivity and phase behavior of the XUV mirror used in the experiment. The reflectivity curve is already the multiplication with the transmission curve of a 150 nm Zr foil, added in the experiment to suppress the fundamental laser radiation. Measurements at the PTB at BESSYII in Berlin have shown that the type of manufacturing process for this mirror leads to a shift in the reflectivity towards higher energy in the order of 4% thus the peak reflectivity is supposed to be ~91 eV

Optimized Reflectivity with Thin „High-Z“ Layers

$$\Gamma = \frac{\Delta t_H}{\Delta t_H + \Delta t_L} = \frac{\Delta t_H}{d} \qquad (4.7)$$

$$\tan(\pi \Gamma_{opt}) = \pi \left[\Gamma_{opt} + \frac{\beta_L}{\beta_H - \beta_L} \right] \qquad (4.8)$$

(Vinogradov and Zeldovich, 1977)
(also see Borrmann, 1941)

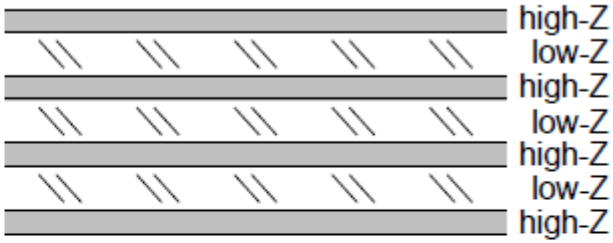

- Sharp interfaces needed for scattering
- Thin high-Z layer to minimize absorption
- Low-Z layer best as a “spacer”

Attwood, D.; Soft X-Ray and Extreme Ultraviolett Radiation, Cambridge University Press, 1999

Influence on Reflectivity

$$R = R_0 \, e^{-\left(\frac{4\pi\sigma \sin\theta_g}{\lambda}\right)^2}$$

where

R_0	smooth surface reflectivity
R	attenuated reflectivity
θ_g	grazing angle of incidence
λ	wavelength of incidence
σ	rms surface roughness

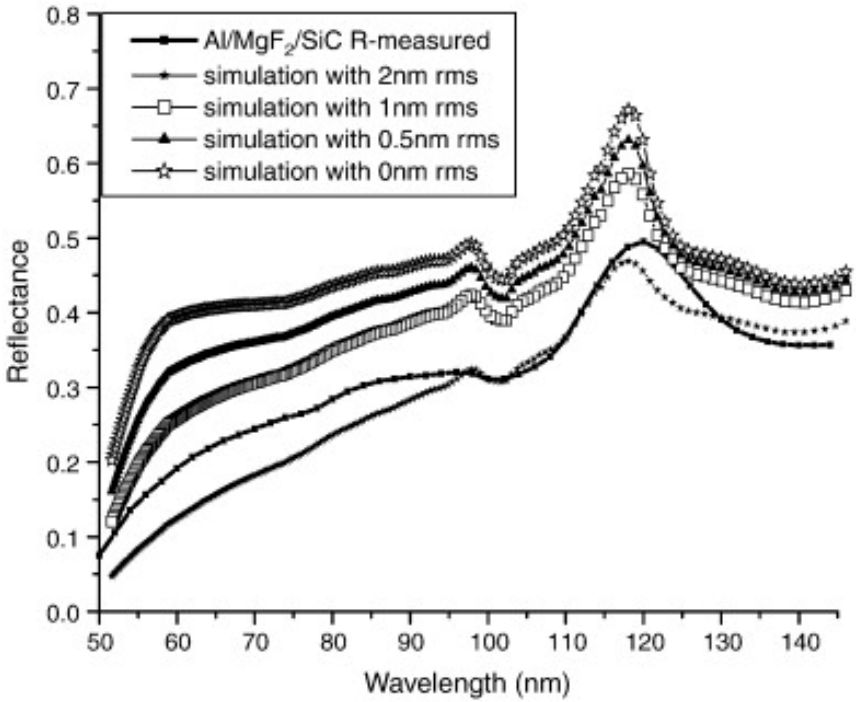

Minghong Yang et al, Thin Solid Films, Volume 517, Issue 2, 28 878-880 (2008)

Optic Simulation Software

http://www.aor.com/

http://www.lambdares.com/education/oslo_edu

http://www.las-cad.com/lascad_images.php

http://www.radiantzemax.com/zemax/

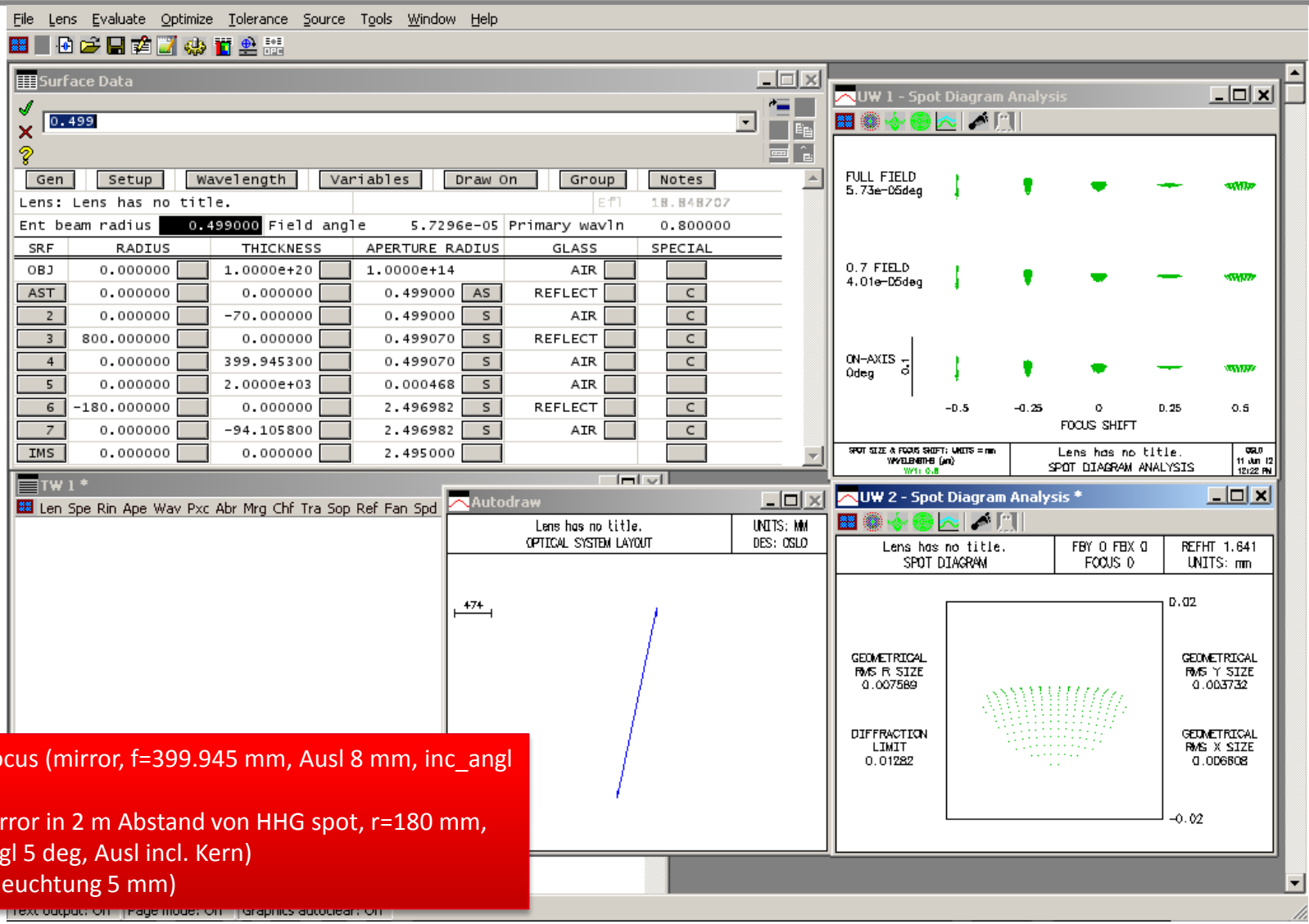

- HHG generating focus (mirror, f=399.945 mm, Ausl 8 mm, inc_angl 6 deg)
- Aussenspiegel (mirror in 2 m Abstand von HHG spot, r=180 mm, Ausl 1 Zoll, inc_angl 5 deg, Ausl incl. Kern)
- Innenspiegel (Ausleuchtung 5 mm)

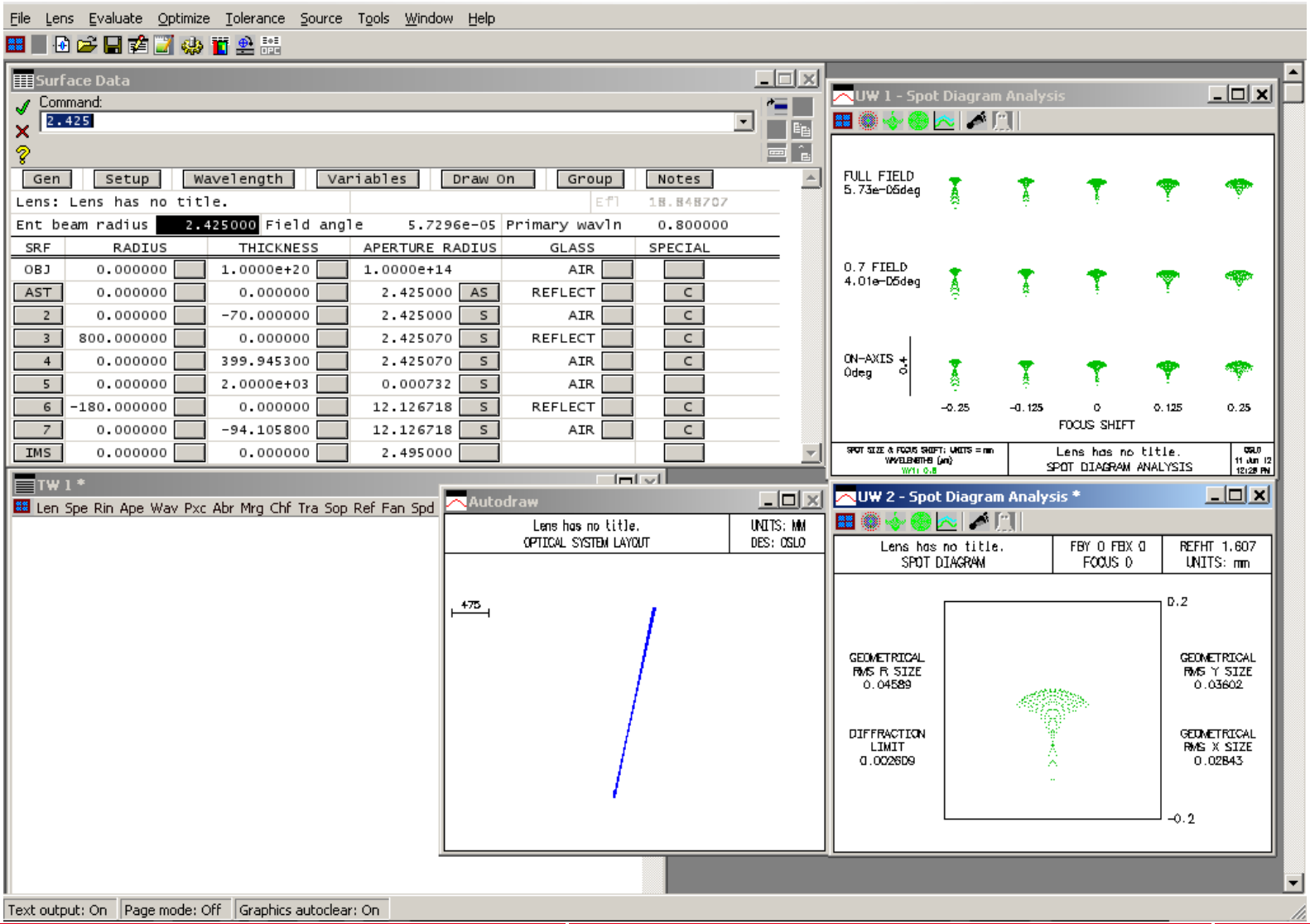
File Lens Evaluate Optimize Tolerance Source Tools Window Help
Surface Data
Command:
2.425
Gen Setup Wavelength Variables Draw On Group Notes
Lens: Lens has no title.
Ent beam radius 2.425000 Field angle 5.7296e-05 Primary wavln 0.800000
SRF RADIUS THICKNESS APERTURE RADIUS GLASS SPECIAL
OBJ 0.000000 1.0000e+20 1.0000e+14 AIR
AST 0.000000 0.000000 2.425000 AS REFLECT C
2 0.000000 -70.000000 2.425000 S AIR C
3 800.000000 0.000000 2.425070 S REFLECT C
4 0.000000 399.945300 2.425070 S AIR C
5 0.000000 2.0000e+03 0.000732 S AIR
6 -180.000000 0.000000 12.126718 S REFLECT C
7 0.000000 -94.105800 12.126718 S AIR C
IMS 0.000000 0.000000 2.495000
UW 1 - Spot Diagram Analysis
FULL FIELD
5.73e-05deg
0.7 FIELD
4.01e-05deg
ON-AXIS
0deg
-0.25 -0.125 0 0.125 0.25
FOCUS SHIFT
Lens has no title.
SPOT DIAGRAM ANALYSIS
TW 1 *
Len Spe Rin Ape Wav Pxc Abr Mrg Chf Tra Sop Ref Fan Spd
Autodraw
Lens has no title.
OPTICAL SYSTEM LAYOUT
UNITS: MM
DES: OSLO
4.75
UW 2 - Spot Diagram Analysis *
Lens has no title.
SPOT DIAGRAM
FBY 0 FBX 0
FOCUS 0
REFHT 1.607
UNITS: mm
GEOMETRICAL RMS R SIZE 0.04589
GEOMETRICAL RMS Y SIZE 0.03602
DIFFRACTION LIMIT 0.0026D9
GEOMETRICAL RMS X SIZE 0.02843
0.2
-0.2
Text output: On
Page mode: Off
Graphics autoclear: On

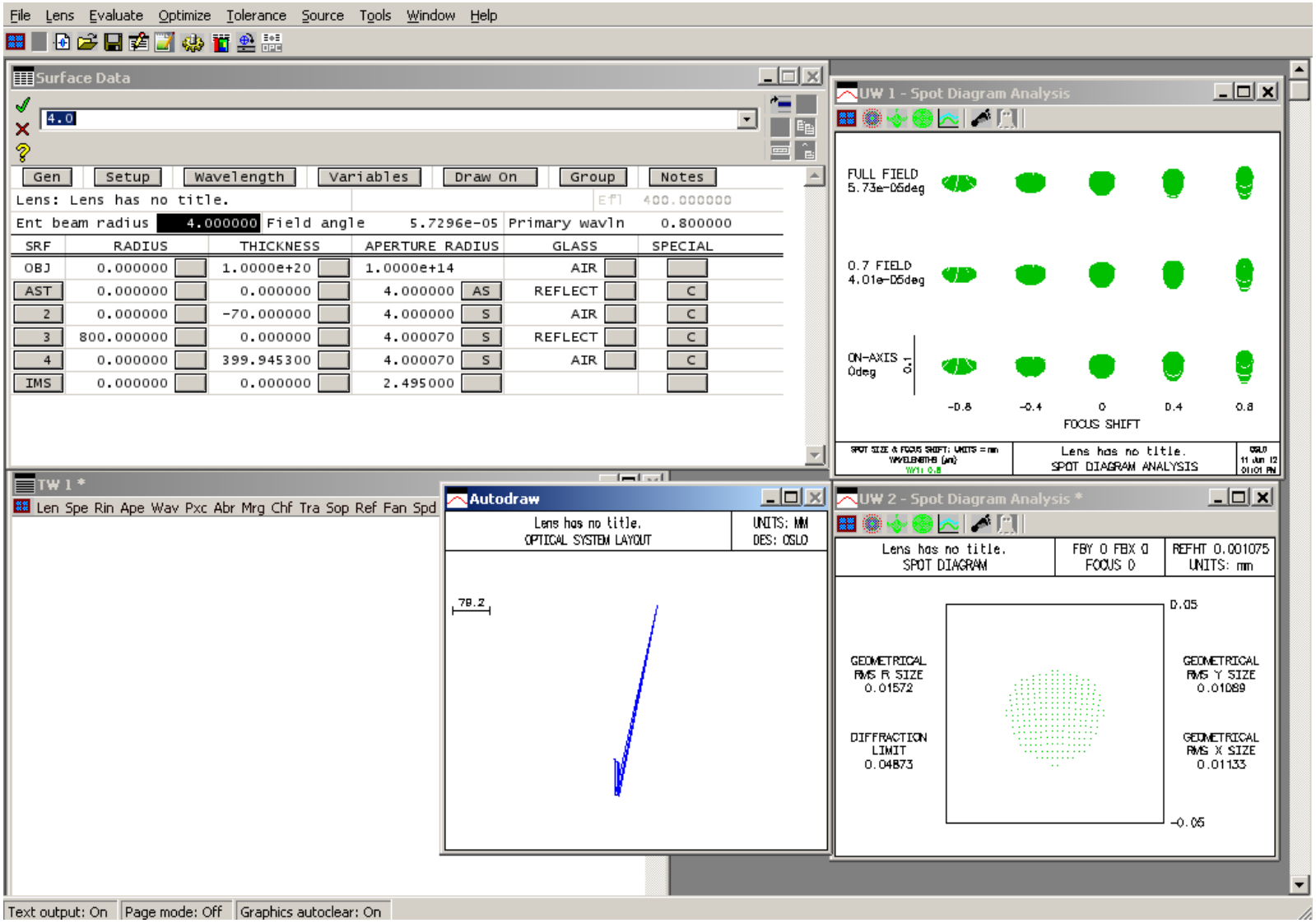
File Lens Evaluate Optimize Tolerance Source Tools Window Help
Surface Data
4.0
Gen Setup Wavelength Variables Draw On Group Notes
Lens: Lens has no title.
Ent beam radius 4.000000 Field angle 5.7296e-05 Primary wavln 0.800000
SRF RADIUS THICKNESS APERTURE RADIUS GLASS SPECIAL
OBJ 0.000000 1.0000e+20 1.0000e+14 AIR
AST 0.000000 0.000000 4.000000 AS REFLECT C
2 0.000000 -70.000000 4.000000 S AIR C
3 800.000000 0.000000 4.000070 S REFLECT C
4 0.000000 399.945300 4.000070 S AIR C
IMS 0.000000 0.000000 2.495000
UW 1 - Spot Diagram Analysis
FULL FIELD
5.73e-05deg
0.7 FIELD
4.01e-05deg
ON-AXIS
0deg
-0.8 -0.4 0 0.4 0.8
FOCUS SHIFT
Lens has no title.
SPOT DIAGRAM ANALYSIS
TW 1 *
Len Spe Rin Ape Wav Pxc Abr Mrg Chf Tra Sop Ref Fan Spd
Autodraw
Lens has no title.
OPTICAL SYSTEM LAYOUT
UNITS: MM
DES: OSLO
78.2
UW 2 - Spot Diagram Analysis *
Lens has no title.
SPOT DIAGRAM
FBY 0 FBX 0
FOCUS 0
REFHT 0.001075
UNITS: mm
0.05
GEOMETRICAL
RMS R SIZE
0.01572
GEOMETRICAL
RMS Y SIZE
0.01089
DIFFRACTION
LIMIT
0.04873
GEOMETRICAL
RMS X SIZE
0.01133
-0.05
Text output: On
Page mode: Off
Graphics autoclear: On

Additional Sources from the WWW:

- 2nd EIROforum School on Instrumentation: X-ray Optics for Synchrotron Radiation Beamlines
- David Attwood; Soft X-Rays and Extreme Ultraviolet Radiation
  http://www.youtube.com/course?list=PL6151C515014FBADA
- Franz Kärtner: Ultrafast Optics
- Michette, A. G. (1986). *Optical Systems for Soft X Rays*. Boston, MA: Springer US. doi:10.1007/978-1-4613-2223-8

Thank you!

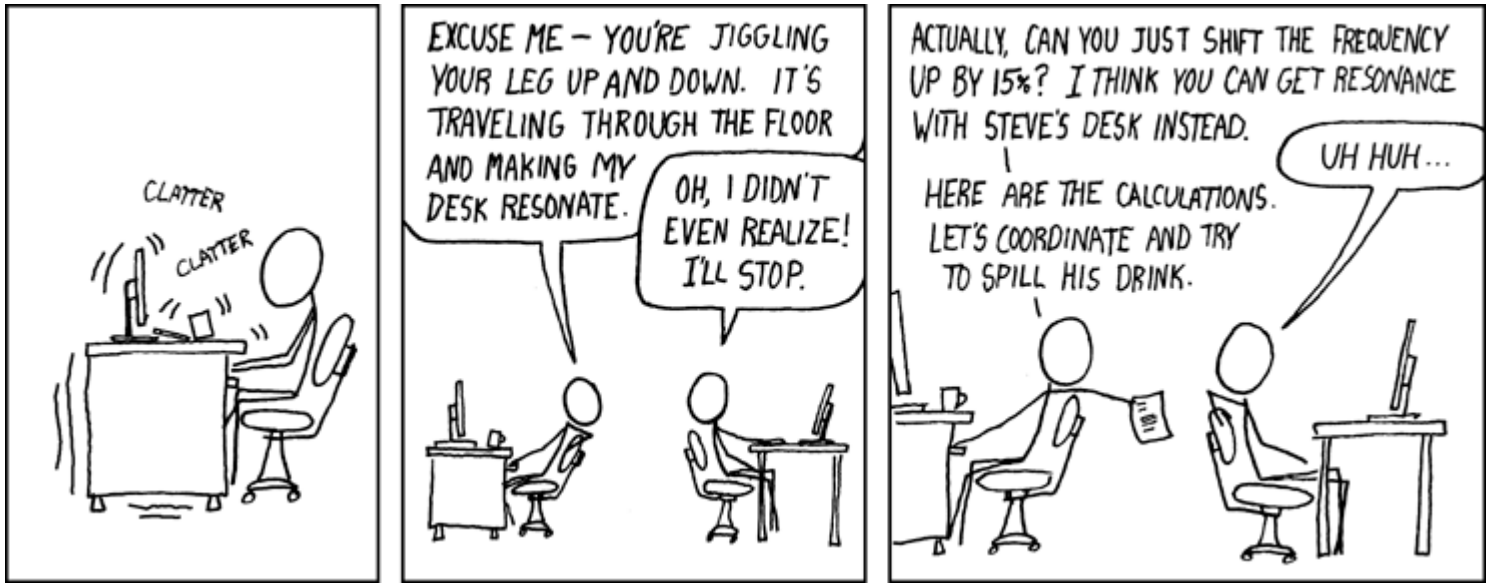
CLATTER
CLATTER
EXCUSE ME – YOU'RE JIGGLING YOUR LEG UP AND DOWN. IT'S TRAVELING THROUGH THE FLOOR AND MAKING MY DESK RESONATE.
OH, I DIDN'T EVEN REALIZE! I'LL STOP.
ACTUALLY, CAN YOU JUST SHIFT THE FREQUENCY UP BY 15%? I THINK YOU CAN GET RESONANCE WITH STEVE'S DESK INSTEAD.
HERE ARE THE CALCULATIONS. LET'S COORDINATE AND TRY TO SPILL HIS DRINK.
UH HUH...